DEFENSE RESEARCH LABORATORY

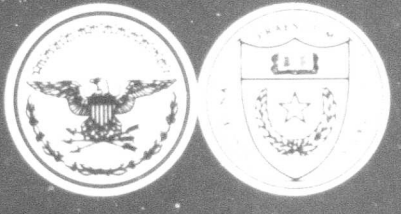

THE UNIVERSITY OF TEXAS · AUSTIN 12, TEXAS

DRL NO-411 CF-2676

AN EXPERIMENTAL INVESTIGATION OF THE EFFECTS OF SEVERAL TYPES OF SURFACE ROUGHNESS ON TURBULENT BOUNDARY LAYER CHARACTERISTICS AT SUPERSONIC SPEEDS

by

Felix W. Fenter
and
W. C. Lyons, Jr.

6 February 1953 Copy No. 62

Contract NOrd-16498
Task UTX-1
Problem UTX-1-A-2

DRL-411, CF-2676
6 February 1958

AN EXPERIMENTAL INVESTIGATION OF THE EFFECTS OF SEVERAL TYPES OF SURFACE ROUGHNESS ON TURBULENT BOUNDARY LAYER CHARACTERISTICS AT SUPERSONIC SPEEDS

by

Felix W. Fenter and W. C. Lyons, Jr.

Defense Research Laboratory
The University of Texas

Austin, Texas

6 February 1958
FWF:WCL:hr

PREFACE

For the past several years, the Defense Research Laboratory of The University of Texas has been engaged in an extensive turbulent boundary layer research program. This theoretical and experimental research has been directed specifically towards determining the effects of both compressibility and surface roughness on the turbulent boundary layer on a flat plate. One phase of the experimental surface roughness program involved boundary layer measurements on a number of surfaces which had been machined with a large variety of roughnesses. These experiments were conducted in the Ordnance Aerophysics Laboratory supersonic wind tunnel and form the subject of this report.

This research effort was supported by the U. S. Navy Bureau of Ordnance as a part of its BUMBLEBEE activity under DRL Contract NOrd-16498. The Applied Physics Laboratory of The Johns Hopkins University acted as the technical sponsor of the program. The authors would like to acknowledge the assistance and support contributed by Dr. M. J. Thompson, Supervisor of the Aeromechanics Division and Associate Director of Defense Research Laboratory. The authors would also like to express their appreciation and gratitude to Messrs. C.J. Stalmach, D. M. Martin, and W. A. Swank of the Aeromechanics Division staff, who assisted with the experimental program and with the extensive numerical computations associated with the data reduction.

Felix W. Fenter
W. C. Lyons, Jr.
6 February 1958

6 February 1958
FWF:WCL:hr

NOMENCLATURE

The following nomenclature is used throughout this report unless otherwise noted:

x = distance along flat plate, measured from leading edge

y = distance normal to plate, measured from surface

U = temporal mean velocity in x-direction

p = absolute pressure

T = absolute temperature

ρ = mass density

M = Mach Number

$R_x = \dfrac{\rho_1 U_1 x}{\mu_1}$ = Reynolds Number

δ = boundary layer thickness

θ = boundary layer momentum thickness

δ^* = boundary layer displacement thickness

G = boundary layer kinetic energy thickness

γ = ratio of specific heats = 1.4 for air

μ = absolute viscosity

D = drag per unit plate width

$C_F = \dfrac{2D}{\rho_1 U_1^2 x}$ = mean skin friction coefficient

$C_d = \dfrac{2\,(D_8 - D_3)}{\rho_1 U_1^2\,(x_8 - x_3)}$ = drag coefficient of insert between survey Stations 3 and 8

ξ = mean diameter of grain-type roughness particles

h = peak-to-valley height of roughness elements

d = spacing or pitch of roughness element

w = width of roughness elements

β = sweepback angle of two-dimensional roughness elements

6 February 1958
FWF:WCL:hr

NOMENCLATURE (Cont'd)

Subscripts:

o = isentropic stagnation conditions in wind tunnel settling chamber

1 = free-stream conditions at outer edge of boundary layer

t = impact stagnation conditions associated with impact probe measurements

6 February 1958
FWF:WCL:hr

TABLE OF CONTENTS

6 February 1958
FWF:WCL:hr

I. INTRODUCTION

The effects of surface roughness on turbulent skin friction received considerable attention during the period from 1930 to 1940 [see Refs. (1), (2), (3), and (4)], but little more was done in this area until recently. This recent revival of interest in the effects of surface roughness may be attributed directly to two factors: (1) the effect of surface roughness on heat transfer as it affects the design of bodies moving through the atmosphere at high speeds, and (2) the important effects of small drag increments on the performance of extremely long range, supersonic, air-breathing vehicles. Fortunately, the early work done at subsonic speeds provided a firm foundation for the current work being done at supersonic speeds.

The Defense Research Laboratory of The University of Texas has been engaged intermittently in studies of surface roughness effects since 1951. As in the case of subsonic flow, the initial work at supersonic speeds utilized grain-type roughness. The results of these initial theoretical and experimental studies [Refs. (5), (6), and (7)] were very gratifying, especially since they indicated that much of the subsonic work could be readily extended to supersonic boundary layers under certain conditions. This grain-type roughness research utilized the DRL boundary layer plate which had previously been used in studies of the turbulent boundary layer on smooth, thermally insulated surfaces at supersonic speeds [Refs. (8) and (9)].

The experiments concerning grain-type roughness reported in Refs. (6) and (10) involved impact probe surveys and limited direct shear stress measurements at a number of stations along the center line of the DRL flat plate, the entire surface of the plate having been coated with various sizes of Aloxite grinding grit. Aloxite grit with mean diameters of 0.00554 inch, 0.00211 inch, 0.00102 inch, and 0.00064 inch were tested in these experimental programs. The results of these tests indicated conclusively that the theoretical equations

reported in Refs.(5) and (7) predicted accurately the effects of surface roughness on turbulent skin friction at Mach Numbers up to at least 2.23. Apparently, these DRL studies represent the major portion of the roughness work done at supersonic speeds as indicated by the surveys presented in Refs. (11) and (12).

Some recent work by Goddard on the effect of grain-type roughness on the drag of bodies of revolution [Ref. (13)] came to the attention of the authors only after the present investigation had been completed.

Unfortunately, grain-type roughness is seldom encountered in practical applications; therefore, it is necessary to extend any comprehensive roughness research program to include the effects of more realistic types of roughness. Here again, the previous work done at subsonic speeds establishes a useful precedent. It was suggested by Schlichting [Ref. (14)] that the roughness of any surface could be described in terms of an equivalent grain size. In other words, the equivalent grain size of a certain roughness is the grain diameter which would produce the same skin friction drag under similar flow conditions. This procedure is very convenient but it has definite limitations which will be briefly discussed later. Consequently, great quantities of subsonic data are available for various types of roughness [Refs. (2), (3), (4), (15), and (16)].

The theoretical and experimental work reported in Refs (5), (6), (7), and (10) indicates conclusively that the procedure of assigning an equivalent grain size to various other roughnesses is equally valid at moderate supersonic speeds. It is convenient to define three regimes of surface roughness: (1) the smooth regime where the surface roughness does not result in a drag increment when compared with perfectly smooth surface, (2) the fully rough regime where the surface shear stress is predominately the result of the turbulent mass interchange caused by the surface roughness and where the fluid viscosity has no appreciable influence on the shear stress, and (3) the intermediate or transition

regime where the surface shear stress is influenced by both fluid viscosity and surface roughness. The great mass of subsonic roughness data indicate that the ratio of equivalent grain size, ξ, to a characteristic dimension of a given roughness, h, is constant if the surface is fully rough. Therefore, one simple experimental test of a given roughness geometry can establish a value of ξ/h which is always valid for fully rough surfaces.

This simple procedure does not hold for the transition regime, and no simple, clearcut method has been devised for treating this roughness regime. For this reason, the characteristic dimension of all roughnesses in the current program was chosen to be the peak-to-valley height, and this dimension was always relatively large - equal to or greater than 0.005 inch. Despite this large height used in these tests, the distribution density of the roughness elements was often varied in such a way as to make the equivalent grain size, in some cases, very small. Therefore, the results of these tests should be extrapolated with caution.

The initial test in the current program utilized the previously mentioned DRL boundary layer plate which was mounted in the test section of the Ordnance Aerophysics Laboratory supersonic wind tunnel. The test Mach Number was M = 2.77. For this test, the entire upper surface of the plate was coated with spherical beads which were approximately 0.004-inch diameter. The purpose of this test was to compare the drag of smooth spherical roughness elements with the drag of the irregular grain-type roughness ordinarily used. These two types of roughnesses have been described by Thompson at DRL as being respectively of the "mole-hill type" and the "Rocky Mountain type" [Ref. (17)]. The results of this initial test are included in this report.

The major portion of the current program utilized the same boundary layer plate which was modified to accommodate large inserts in its test surface. These inserts were machined with various types of roughness, and the drag on each insert was measured by means of impact probe surveys of the boundary layer. The modified boundary layer plate and the inserts are described in detail in the

following section of this report. It was originally planned to test an extensive series of inserts which would involve a systematic variation of several roughness geometric parameters. Unfortunately, the decision to cease operations at the OAL supersonic wind tunnel occurred when this program was approximately half finished; consequently, the following data are in many respects, fragmentary and difficult to interpret. Nevertheless, it is believed that these data are useful and may form the foundation for a more extensive future investigation. This report contains a detailed description of the apparatus and the experimental procedure as well as a discussion of the final results.

6 February 1958
FWF:WCL:hr

II. DESCRIPTION OF EXPERIMENTS

The data presented in this report can be divided into two categories, as was previously mentioned. The first category consists of data obtained using a spherical roughness with a mean diameter of 0.00412 inch. These data were obtained from tests in which the surface of a thermally insulated flat plate was completely covered with this spherical roughness. A complete discription of this flat plate is presented in Ref. (8). The velocity distribution and the Mach Number distribution through the boundary layer and normal to the surface of the plate is presented in Table I for seven stations located along the longitudinal center line of the plate. Table II is a summary of the boundary layer characteristics obtained at each of these seven stations for the spherical roughness.

The second category of data was obtained by modifying the flat plate mentioned in the preceding paragraph. Since this report is concerned primarily with the data in this second category, a more thorough discussion of the model, equipment, and procedures utilized will be presented in the following sections. This second category consists of data obtained from tests utilizing both uniform grain-type roughness and machined-type roughness on inserts mounted in the modified flat plate.

A. Wind Tunnel

The data in both categories previously mentioned were obtained from tests conducted in the Ordnance Aerophysics Laboratory Supersonic Wind Tunnel at Daingerfield, Texas. This wind tunnel uses interchangeable nozzle blocks for varying the test section Mach Number. The tests utilizing the spherical roughness were conducted at a Mach Number of 2.77. The remainder of the data reported was obtained for a Mach Number of 2.23. The test section of this wind tunnel is rectangular in cross section, with a height of 27-1/2 inches and a width of 19 inches. A more detailed description of this wind tunnel is presented in Ref. (18). Figure 1 is a drawing of the test section of this wind tunnel with the flat plate installed in it.

6 February 1958
FWF:WCL:hr

B. Flat Plate Model

The model used in these tests was the flat plate described in Ref. (8), modified to accommodate thin aluminum inserts as shown in Fig. 1. The plate was 19-inches wide and 36-inches long, with a maximum thickness of approximately 0.916 inches. The plate was made of Monel. The leading edge of the plate was beveled on the under side to form a sharp, single wedge with a 6.7 degree angle. At a distance of 3/4 inches from the leading edge, an area of the plate was knurled, using a standard 1/4-inch width knurling tool. This knurled area spanned the width of the plate. The peaks of the knurls protruded approximately 0.005 inches above the surface of the plate. This knurled strip was machined into the plate for the purpose of locating the point of transition from laminar to turbulent flow near the leading edge of the plate.

Three static pressure orifices were located along the center line on the forward portion of the plate. The location of these orifices are shown in Fig. 1. Two holes, 1-5/16 inches in diameter, were also located along the center line of the plate. One was 13.80 inches from the leading edge, while the other was 33.80 inches from the leading edge. These two holes accommodated a total pressure probe which was used to survey the boundary layer normal to the surface of the plate at these two stations. This probe is described in another section of this report. Solid plugs whose surfaces were flush with the surface of the plate could be inserted into either of these two holes when they were not occupied by the probe.

An area in the center of the plate, 15-inches wide and 24-inches long was machined to a depth of 5/16 inch. This was done to allow thin inserts to be installed in this larger Monel plate. A description of these inserts is presented in the following section. Figure 2 is a drawing of the plate and insert installed in the wind tunnel, showing a typical test set-up.

6 February 1958
FWF:WCL:hr

C. Roughness Inserts

In order that a variety of types of surface roughness could be tested utilizing the same basic plate, removable aluminum inserts were used. Figures 1 and 3 are drawings of these inserts. The inserts were approximately 15-inches wide and 24-inches long. The nominal thickness was 1/4 inch; however, this varied from one insert to another.

Eighteen holes, distributed throughout the under side of each insert, were drilled and tapped to receive standard 1/4" - 20 Allen head screws. These screws were part of an adjusting scheme designed to position the surface of the inserts flush with the surface of the Monel plate. Figure 3 indicates the general location of these points of adjustment and also shows a detailed sketch of one of the adjusting screws. The inside screw, labeled "locking screw", holds the insert in the main plate. The "adjusting screw" permits the insert to be raised or lowered with respect to the surface of the main plate. Finally, a cap was used to pressure seal the bottom of the main plate from the cavity between the main plate and the under side of the insert.

Each insert was provided with a rubber sealing cord which extended across the width of the plate. This cord was installed in the leading edge of each insert, midway between the upper and lower surfaces. This cord prevented any flow from occurring between the leading edge of an insert and the main plate which might disturb the normal boundary layer.

A total of sixteen inserts was tested, and each insert was numbered from 1 to 16. Table III, with the aid of Fig. 4, lists all of these inserts and designates the type of surface roughness associated with each insert. The various pertinent dimensions associated with each roughness are also given in Table III. Insert No. 1 was machined and then hand rubbed until the surface was very smooth. When installed in the main plate, the entire configuration was a

smooth flat plate, just as the main plate had been before its modification. Inserts Nos. 2, 3, 4, and 5 had surfaces which were covered with a uniform size grit, each of different mean diameters. These first five inserts formed a series of control surface roughnesses to which the machined surface roughnesses of the other inserts could be compared.

Inserts Nos. 6 through 16 had surfaces on which various machined type roughnesses had been formed. Insert No. 6 had a 0.020-inch, forward-facing step machined across its span. Inserts Nos. 7 and 8 had surfaces in which spherical indentures had been machined. Inserts Nos. 9 through 13 had V-grooves machined normal to the direction of flow in their surfaces. Inserts Nos.14 and 15 had V-grooves, swept back with respect to the direction of flow, machined into their surfaces. Lastly, the surface of insert No. 16 was covered with protruding rivet heads. All of the various type roughnesses started at a line 2.840 inches from the leading edge of the insert and extended over the entire insert surface between this line and the trailing edge. Figure 5 is a photograph of six typical, machined roughness inserts.

D. Probe Assembly

The impact pressure probe utilized in these test was the same probe as described in Refs. (8), and (9). Details of this probe may be seen in Fig. 6. The tip of the probe consisted of 0.020-inch O.D. stainless steel tube, with a 0.010-inch bore. This tube was fastened to a larger 0.035-inch O.D. stainless steel tube which, in turn, ran through a double wedge which supported the probe. Plastic tubing was connected to this 0.035-inch O.D. tubing and was led outside the wind tunnel through a series of pressure sealed plugs. A screw mechanism was connected through two bevel gears and a flexible shaft to a micrometer located outside of the wind tunnel. The micrometer head could be rotated to actuate the probe and to indicate the location of the tip of the probe above the surface of the plate during a test. The probe can be seen installed in the plate in Fig. 7.

E. Test Procedure

The procedure of test preparation and the actual testing itself was slightly different in the case of the spherical roughness from that used for the insert tests. Only a brief discussion will be given for the spherical roughness test procedures. The method used in applying the spherical roughness to the plate and the procedure for installing the plate in the wind tunnel was identical to that presented in Ref. (6). In general, the procedure for conducting the wind tunnel tests was also the same as that outlined in Ref. (6). In the spherical roughness tests, impact-pressure surveys at seven stations along the center line of the plate were made. Direct measurements of the surface shear stress, utilizing skin friction balances as described in Ref. (6), were not performed. The impact-pressure surveys were started at the aft-most station and progressed forward in succeeding runs. Plugs were installed in the survey station holes that were not occupied by the probe. Between twenty and thirty points were obtained at each station, depending upon the thickness of the boundary layer.

In order that the tip of the probe could be located accurately at different positions above the surface of the plate, it was necessary to first locate it when in contact with the surface of the plate. The method used to accomplish this involved noting the impact pressure reading while the wind tunnel was running. A very rapid change in the impact pressure could be observed as the probe was retracted toward the surface of the plate, due to the large velocity gradient in the boundary layer in the neighborhood of the surface of the plate. A minimum impact pressure reading was observed when the tip of the probe made contact with the surface of the plate. Further actuation of the probe mechanism caused no further change in the pressure reading. Since the probe tip was then on the surface of the plate, any further actuation of the mechanism simply resulted in "wind-up" in the flexible shaft. By rotating the micrometer head very slowly and carefully noting the micrometer reading when this minumum pressure was initially attained, the location of the tip of the probe on the surface could be accurately accomplished. This method proved to be reliable and repeatable.

6 February 1958
FWF:WCL:hr

Application of the uniform grit to the surface of four of the inserts was accomplished exactly as described in Ref. (6). The inserts were first sprayed with a mixture of clear varnish and Japan drier until a very thin coating was obtained. The grit was then applied by means of a flocking gun until the surface was evenly and completely covered with one thin layer of the grit. This coating was allowed to dry for at least one day before testing.

The surfaces of the inserts which contained the spherical, indenture-type roughness were formed on a horizontal milling machine, using a specially ground tool. The cutting end of the tool was designed so that the proper diameter and depth of the indentures could be obtained.

The surfaces of the inserts which contained the V-groove roughnesses were formed on a shaper. Again, a specially ground tool which gave a V-groove whose bottom vertex angle was 90 degrees was used. The insert whose surface was smooth was first machined on the shaper and then hand rubbed with fine emory paper until a very smooth surface was attained.

The inserts, containing the rivets were formed simply by drilling the correct sized holes at the proper location and then setting rivets in each of these holes.

The installation of the main plate in the wind tunnel was accomplished using the same procedure as described in Ref. (6). The inserts were installed in the plate while it remained in the wind tunnel, and the insert surfaces adjusted flush with the main plate surface by using the adjusting screws previously described. By using a surface dial indicator, the insert surfaces could be checked to assure that they coincided with the main plate surface at the edges of the inserts. The center portion of the inserts were then adjusted so that the entire surface of a given insert and the surface of the main plate lay in the same plane.

6 February 1958
FWF:WCL:hr

Two U-tube manometers were utilized in these tests. One was used to read the impact pressure indicated by the probe, while the other manometer indicated the static pressure in the stilling chamber of the wind tunnel. Atmospheric pressure was used as a reference in measuring both of these pressures. Both of these pressures were read for each data point taken. The test of each insert involved a boundary layer survey at the rear station which will be referred to as Station 8. Since the boundary layer did not change appreciably from one test to the next at the forward survey station (Station 3), surveys at Station 3 were made at representative intervals only and not for every insert tested.

6 February 1958
FWF:WCL:hr

III. DATA REDUCTION

The procedure utilized to reduce the data from these tests coincided very closely with that utilized in Ref. (6). No direct measurements of the local shear stress on the surface of the plate were made; so that consequently, no procedure was necessary for reducing this type of data. The following sections will present a brief discussion of the data reduction procedures used for the tests described in this report.

A. Free-Stream Conditions

This section, which is concerned with the determination of the free-stream flow conditions, applies equally to the tests using the spherical roughness and the roughness inserts. Since both the wind tunnel stilling chamber pressure, p_o, and temperature, T_o, were measured for each data point, free-stream conditions in the wind tunnel test section were obtained by means of the isentropic flow relations.

Using the impact pressure reading, p_{t_1}, obtained with the probe fully extended and outside of the boundary layer, and the pressure obtained in the tunnel stilling chamber, p_o, the free-stream Mach Number, M_1, was determined using the tables in Ref. (19). Having established the free-stream Mach Number at each station, the free-stream static pressure, p_1, at each station may be determined by using Ref. (19) and knowing the tunnel stilling chamber pressure. Having measured the stilling chamber temperature, the free-stream ambient temperature, T_1, and density, ρ_1, were determined at each station, using the previously determined value for the free-stream Mach Number and the tables in Ref. (19). The free-stream velocity, U_1, could then be determined using the

the following equation

$$U_1 = M_1 \sqrt{\gamma R_g T_1} \qquad (1)$$

where R_g is the gas constant defined by the equation of state for a perfect gas. The Reynolds Number, R_x, at any particular survey station at a distance x from the leading edge, is obtained as:

$$R_x = \frac{\rho_1 U_1 x}{\mu_1} \qquad (2)$$

Values of the viscosity, μ_1, were determined from Ref. (20).

B. Impact Pressure Probe Data

The methods used and the assumptions involved in reducing the impact pressure data to final form are as follows: (1) the static pressure is constant through the boundary layer at any given streamwise location, i.e., the static pressure gradient normal to the plate surface is zero; and (2) the boundary layer flow is isoenergetic, i.e., the total energy is constant throughout the layer. The justifications for making these two assumptions are given in Refs. (6) and (8).

Using the static pressure previously determined for each station and the impact pressure measured with the probe, the local Mach Number, M, for each point in the boundary layer was determined using the Rayleigh formula.

$$\frac{p_1}{p_t} = \frac{\left(\frac{2\gamma}{\gamma+1} M^2 - \frac{\gamma-1}{\gamma+1}\right)^{\frac{1}{\gamma-1}}}{\left(\frac{\gamma+1}{2} M^2\right)^{\frac{\gamma}{\gamma-1}}} \tag{3}$$

The Mach Numbers for various values of the ratio p_1/p_t are tabulated in Ref. (19). The temperature variation within the boundary layer based on the assumed isoenergetic flow was obtained from the following relation:

$$\frac{T}{T_1} = \frac{\left(1 + \frac{\gamma-1}{2} M_1^2\right)}{\left(1 + \frac{\gamma-1}{2} M^2\right)} \tag{4}$$

The velocity ratio was then computed from the Mach Number and temperature ratios by means of the following equation:

$$\frac{U}{U_1} = \frac{M}{M_1} \sqrt{\frac{T}{T_1}} \tag{5}$$

The Mach Number and velocity distributions for each of the seven stations surveyed during the spherical roughness tests are presented in Table I. The Mach Number and velocity distributions for stations at which surveys were run on each of the roughness inserts are presented in Table IV. For constant static pressure across the boundary layer, the density is given by:

$$\frac{\rho}{\rho_1} = \frac{T_1}{T} \tag{6}$$

The boundary layer momentum thickness, θ, is defined by:

$$\theta = \int_0^{\delta} \frac{\rho U}{\rho_1 U_1} \left(1 - \frac{U}{U_1}\right) dy \qquad (7)$$

where δ represents the boundary layer thickness, and y is measured normal to the surface of the plate. Values of θ at each survey station were obtained by carrying out numerically the integration indicated in Eq. (7).

The mean skin friction coefficient, C_F, for a flat plate is given by:

$$C_F = \frac{2\theta}{x} \qquad (8)$$

where x is the length measured from the leading edge of the plate back to a particular station. A summary of the boundary layer characteristics for a spherical roughness (M, R, θ, C_F, etc.) is presented in Table II. A summary of boundary layer characteristics for Station 8 on each of the sixteen inserts is presented in Table V.

C. Equivalent Grain-Size Determination

The mean diameter, ξ, of each of the four uniform grain sizes tested (Insert Nos. 2, 3, 4, and 5) was determined by measuring, by means of a microscope, approximately 200 grains of each size. Using these average values of ξ, a Reynolds Number based on grain diameter was computed for each insert from the equation

$$R_\xi = \frac{\rho_1 U_1 \xi}{\mu_1} \qquad (9)$$

6 February 1958
FWF:WCL:hr

Using the average value of the momentum thickness, θ_3, measured at Station 3, an effective length from the leading edge of the plate back to Station 3 was computed for various values of R_ξ using the equations presented in Ref. (5). Using this effective length to adjust the actual length from the leading edge of the plate back to Station 8, a value for θ_8 was theoretically computed for the various values of R_ξ previously used. From these theoretical values of θ_8 and θ_3, a drag coefficient, C_d, was determined, which is defined as:

$$C_d = \frac{D}{1/2\ \rho_1 U_1^2 \left(x_8 - x_3\right)} \tag{10}$$

or

$$C_d = \frac{2\left(\theta_8 - \theta_3\right)}{\left(x_8 - x_3\right)} \tag{11}$$

Similarly, a value for the drag coefficient, C_{d_s}, for a smooth plate ($R_\xi = 0$) was computed from the equations in Ref. (8). In Fig. 8 the theoretical values of C_d/C_{d_s} are plotted as a function of R_ξ, as shown by the solid line. Also shown on this plot are values of C_d/C_{d_s} obtained experimentally from the uniform, grain-roughness inserts and from two other programs in which similar grain-roughness data were obtained. The data from these other two programs were obtained by covering the complete plate with the grit rather than having a smooth portion of the plate in front of the roughness, as was the case in the insert tests. Consequently, these data were theoretically corrected before they were plotted in Fig. 8. This correction procedure utilized the theory of Ref. (5) to account for the additional drag increment caused by the roughness forward of Station 3. It can be seen that excellent agreement between theory and experiment was obtained.

6 February 1958
FWF:WCL:hr

Figure 8 was used to determine the equivalent grain roughness of the various inserts. The values of C_d/C_{d_s} associated with each insert yielded a value of ξ, which is defined as the equivalent grain diameter of each particular roughness. These values of ξ as well as ξ/h are tabulated in the summary of data given in Table V.

6 February 1958
FWF:WCL:hr

IV. DISCUSSION OF RESULTS

The various errors associated with impact pressure probe surveys have been discussed in detail in previous reports dealing with similar measurements [Refs. (6), (8), and (9)]. The specific errors associated with the pressure measurements in these particular tests have been estimated as follows:

$$\frac{p_t}{p_o} \text{ — } \pm 0.0008$$

$$M \text{ — } \pm 0.0020$$

$$\frac{U}{U_1} \text{ — } \pm 0.0063$$

As a result of these considerations it is believed that the momentum thickness measurements are accurate within 3%. All estimates of accuracy were conservative and assumed to be cumulative; therefore, the actual accuracy of the measurements is probably better than 3% in most cases.

The mean skin friction coefficients measured for the spherical roughness are compared with the theory of Ref. (5) in Fig. 9, and a typical velocity profile is compared with the smooth plate profile in Fig. 10. No effort was made in this case to determine an equivalent grain roughness since it was suspected that the spheres would give essentially the same results as the irregular grains. Also, no effort was made to correct these data to allow for the fact that some laminar and transitional flow existed near the leading edge of the plate. Since the theory deals only with boundary layers that are initially turbulent, agreement between theory and experiment should not be anticipated except at large Reynolds Numbers (say, greater than 10^7) where the leading edge effect becomes very small.

The good agreement between theory and experiment in Fig. 9 indicates that the ratio ξ/h is essentially unity in this case. It should be noted that this result is not necessarily in conflict with the results obtained by Schlichting [Ref. (14)] in subsonic flow. Schlichting obtained a value of ξ/h of 0.62 for spheres arranged in maximum density of distribution. His spheres were attached to the plate only at the point of tangency, and the air was free to flow in the interstices between the undersides of the spheres. In the present case, the spheres were bonded to the plate by being partially imbedded in a layer of varnish. It is believed that the resulting surface bore little relation to Schlichting's surface. In any event, the tiny glass spheres used in the current test resulted in a skin friction coefficient which was not measurably different from the coefficient of grain-type roughness of the same size.

The velocity profiles obtained at Station 8 for all inserts are shown in Figs. 11 through 16. Each of these figures contains an appropriate reference profile for comparison purposes. Figure 11 compares the velocity profiles obtained for each degree of grain-type roughness with a corresponding smooth surface profile. It can be seen that increasing grain roughness size results in increased boundary layer thickness without changing the basic character of the profile. This trend is, of course, predicted by the theory of Ref. (6).

The velocity profiles obtained for V-grooves normal to the air stream with varying densities of distribution are compared with a smooth profile in Fig. 12. The surface with full density V-grooves results in a thicker boundary layer in accordance with the value of $\xi/h = 0.62$ associated with this roughness. Increasing values of d/h result in velocity profiles which approach smooth profiles, as would be anticipated. The variation of the velocity profile with sweepback angle of the full density V-grooves is shown in Fig. 13. It can be seen that increasing sweepback results in a thinner boundary layer for a given roughness size. This result would, of course, be anticipated by considering the limiting case of 90° sweepback.

6 February 1958
FWF:WCL:br

The velocity profiles obtained with the two distribution densities of spherical indentations (dimples) are compared with a smooth profile in Fig. 14. It can be seen that the nature of the velocity profile is drastically affected by this type of roughness. Reference to Table V indicates that neither density of distribution resulted in a drag increase over that of a smooth plate in spite of this change in velocity profile. It is regrettable that dense distributions of this type roughness could not be tested as originally planned. It is significant to note that the boundary layer thickness was not appreciably increased by the spherical indentations, which is consistent with the lack of drag increase.

The velocity profile obtained from the insert with rivet heads is compared with a smooth profile in Fig. 15. It can be seen that this protruding roughness changed the character of the velocity profile in a manner similar to the indentations. Contrary to the indentations, the rivet heads caused a large increase in boundary layer thickness which is consistent with the large drag rise listed in Table V. A careful study of the static pressures along the insert and of the free-stream impact pressures indicated that the wave-drag of the rivet heads was negligible, and all the drag could be accounted for in the momentum deficit of the boundary layer.

The velocity profile behind the forward-facing step is compared with the smooth profile in Fig. 16. It can be seen that this relatively large surface discontinuity had little effect on the velocity profile. The boundary layer thickness was not appreciably increased, which is consistent with the fact that the drag coefficient of the step was negligibly small when based on the entire insert area as evidenced by Table V. It is believed that this step created a large local disturbance, but the boundary layer had returned to an equilibrium state by the time it reached the survey station.

Since these data are fragmentary and incomplete, it was not possible to perform a significant amount of interpretation in most cases. The major results of the tests have been tabulated in Table V, and these results can be used, in many cases, for design estimates and approximations. The V-groove family of inserts represents the most nearly complete set of data. The variation of the equivalent grain roughness of V-grooves with density of distribution is shown in Fig. 17. It can be seen that the maximum roughness effect does not correspond to the maximum distribution density. This result is consistent with Schlichting's results for a variety of three-dimensional roughnesses. In fact, the shape of the curve faired through the points in Fig. 17 has the same general shape as a curve faired through a similar plot of Schlichting's data [Ref. (14)] with only the vertical scale being different.

Similarly, the variation of equivalent grain roughness with sweepback angle of V-grooves is shown in Fig. 18. It can be seen that the general effect of sweepback is to decrease the effect of the roughness as previously noted. The curve faired through the data points in Fig. 18 is only qualitative since the correct shape of this curve is not known.

6 February 1958
FWF:WCL:hr

V. CONCLUSIONS

As a result of the experiments described in this report, the following conclusions are made concerning the effects of roughness on the turbulent boundary layer of a thermally insulated flat plate at moderate supersonic speeds:

1. The theory given in Refs. (5) and (7) can be used to predict accurately the skin friction drag of surfaces with uniform grain-type roughness. The roughness does not necessarily have to extend to the leading edge of the surface for an accurate calculation to be made.
2. Uniform surface roughness composed of spherical beads does not affect the boundary layer in a manner significantly different from grain-type roughness, provided that the grains and the spheres are bonded to the surface in a similar manner. Consequently, the theory of Refs. (5) and (7) accurately predicts the effects of spherical roughness elements on skin friction under these conditions. These conclusions are not applicable if the roughness elements become significantly large compared to the boundary layer thickness.
3. The effect of a given type of roughness on turbulent boundary layer characteristics is strongly dependent upon the density of distribution of the roughness elements. These tests indicate that the variation of equivalent grain roughness with distribution density of V-groove is similar in nature to the variation found by Schlichting for various three-dimensional roughnesses. The maximum drag for a given roughness size does not necessarily correspond to the maximum density of distribution.
4. The effect of maximum density V-grooves on turbulent boundary layer characteristics is dependent upon the sweepback angle. The effect of increasing sweepback is to reduce the skin friction drag.

6 February 1958
FWF:WCL:hr

REFERENCES

1. Prandtl, L., and Schlichting, H., "Das Widerstandsgesetz Rauher Platten", Werft Reederei Hafen, Jahrg. 15, Heft1, pp. 1 - 4. January, 1934.

2. Schlichting, H., "Experimental Investigation of the Problem of Surface Roughness," NACA TM-823, April, 1937.

3. Jacobs, W., "Variation in Velocity Profile with Change in Surface Roughness of Boundary," NACA TM-951, September, 1940.

4. Tillmann, W., "Additional Measurements of the Drag of Surface Irregularities in Turbulent Boundary Layers," NACA TM-1299, January 1951.

5. Fenter, F. W., "A Theoretical Analysis of the Effects of Surface Roughness on the Turbulent Boundary Layer in Compressible Flow with Zero Heat Transfer," Report No. DRL-365, CM-824, Defense Research Laboratory, The University of Texas, Austin, Texas, April, 1955.

6. Shutts, W. H., and Fenter, F. W., "Turbulent Boundary Layer and Skin Friction Measurements on an Artificially Roughened, Thermally Insulated Flat Plate at Supersonic Speeds," Report No. DRL-366, CM-837, Defense Research Laboratory, The University of Texas, Austin, Texas, August, 1955.

7. Fenter, F. W., "The Effect of Heat Transfer on the Turbulent Skin Friction of Uniformly Rough Surfaces in Compressible Flow," Report No. DRL-368, CM-839, Defense Research Laboratory, The University of Texas, Austin, Texas, April, 1956.

8. Wilson, R. E., "Characteristics of Turbulent Boundary Layer Flow over a Smooth, Thermally Insulated Flat Plate at Supersonic Speeds," Report No. DRL-301, CM-712, Defense Research Laboratory, The University of Texas, Austin, Texas, June, 1952.

9. Shutts, W. H., Hartwig, W. H., and Weiler, J. E., "Turbulent Boundary Layer and Skin Friction Measurements on a Smooth, Thermally Insulated Flat Plate at Supersonic Speeds," Report No. DRL-364, CM-825, Defense Research Laboratory, The University of Texas, Austin, Texas, January, 1955.

10. Fenter, F. W., "An Investigation of the Threshold Value of Surface Roughness at Supersonic Speeds," Report No. DRL-416, CM-919, Defense Research Laboratory, The University of Texas, Austin, Texas, (to be published).

REFERENCES (CONT'D)

11. Gollos, W. W., "Boundary Layer Drag for Non-Smooth Surfaces," RM-1129, The Rand Corporation, Santa Monica, California, June, 1953.

12. Liepmann, H. W., and Goddard, F. E., "Note on the Mach Number Effect Upon the Skin Friction of Rough Surfaces," Journal of the Aeronautical Sciences, Vol. 24, No. 10, October, 1957.

13. Goddard, F. E., Jr., "Effect of Uniformly Distributed Roughness on Turbulent Skin-Friction Drag at Supersonic Speeds," Report No. 20-113, Jet Propulsion Laboratory, California Institute of Technology, 3 September 1957.

14. Schlichting, H., Boundary Layer Theory, McGraw-Hill Book Co., New York, 1955.

15. Hama, F. R., "Boundary Layer Characteristics for Smooth and Rough Surfaces," Transactions of the Society of Naval Architects and Marine Engineers, Vol. 62, 1954.

16. Ambrose, H. H., "The Effect of Character of Surface Roughness on Velocity Distribution and Boundary Resistance", Final Report, Contract Nonr 811(03), Engineering Experiment Station, The University of Tennessee, Knoxville, Tennessee (undated).

17. "Minutes of Sixteenth Regular Meeting," Bumblebee Aerodynamics Panel, Silver Spring, Maryland, 1-2 August 1951, APL/JHU/TG 14-13, Applied Physics Laboratory, The Johns Hopkins University, Silver Spring, Maryland, 1 November 1951, p. 14. (CONFIDENTIAL)

18. Townsend, C. N., "Handbook for Testing at the OAL Supersonic Wind Tunnel," OAL Report No. 46, April, 1949.

19. Riise, H. N., "Compressible Flow Tables for Air in Increments of 0.001 in Mach Number," Publication No. 27, Jet Propulsion Laboratory, California Institute of Technology, Pasadena 3, California, 7 August 1954.

20. Tables of Thermal Properties of Gases, U. S. Department of Commerce, National Bureau of Standards Circular 564, Washington, D. C., November, 1955.

This report has been distributed in accordance with the list for Aerodynamics contained in APL/JHU, TG 8 - 11, dated November, 1953.

TABLE I

BOUNDARY LAYER MACH NUMBER AND VELOCITY DISTRIBUTIONS FOR SPHERICAL ROUGHNESS

TUNNEL MACH NUMBER = 2.77 α = -1.25° ξ = .00412 in.

STATION 2	STATION 3	STATION 4
x = 0.638 ft.	X = 0.971 ft.	x = 1.304 ft.
P_o = 96.94 in. Hg.	P_o = 96.56 in. Hg.	P_o = 95.70 in. Hg.
T_o = 119°F	T_o = 121°F	T_o = 121°F
M_1 = 2.699	M_1 = 2.702	M_1 = 2.702

y-in.	M	U/U_1	y-in.	M	U/U_1	y-in.	M	U/U_1
.0090	1.168	.6014	.0090	1.066	.5584	.0090	1.107	.5757
.0110	1.171	.6023	.0130	1.133	.5865	.0110	1.164	.5992
.0160	1.245	.6316	.0180	1.191	.6100	.0130	1.200	.6137
.0210	1.316	.6587	.0230	1.221	.6221	.0176	1.241	.6297
.0260	1.390	.6856	.0280	1.268	.6402	.0230	1.278	.6440
.0310	1.422	.6976	.0330	1.332	.6642	.0289	1.324	.6612
.0360	1.513	.7278	.0382	1.380	.6818	.0339	1.363	.6756
.0461	1.638	.7675	.0430	1.417	.6949	.0388	1.402	.6893
.0662	1.868	.8325	.0480	1.437	.7017	.0438	1.429	.6980
.0760	1.950	.8536	.0580	1.515	.7280	.0543	1.473	.7140
.0860	2.052	.8781	.0680	1.593	.7533	.0638	1.538	.7355
.0960	2.183	.9072	.0780	1.642	.7684	.0738	1.569	.7454
.1060	2.263	.9238	.0882	1.735	.7958	.0840	1.639	.7673
.1162	2.392	.9487	.0982	1.794	.8124	.0938	1.684	.7810
.1410	2.592	.9834	.1234	1.973	.8587	.1038	1.727	.7935
.1662	2.673	.9961	.1486	2.157	.9012	.1138	1.792	.8116
.1910	2.693	.9992	.1733	2.333	.9372	.1390	1.926	.8470
.2162	2.696	.9996	.1980	2.484	.9647	.1638	2.052	.8775
.2410	2.699	1.0000	.2230	2.611	.9860	.1888	2.176	.9052
			.2480	2.670	.9952	.2138	2.298	.9303
			.2730	2.688	.9978	.2388	2.415	.9523
			.2980	2.696	.9992	.2638	2.521	.9710
			.3230	2.697	.9992	.3140	2.656	.9929
			.3730	2.701	.9998	.3638	2.694	.9988
			.8220	2.702	1.0000	.4138	2.692	.9984
						.4638	2.696	.9991
						.8238	2.702	1.0000

TABLE I (CONT'D)

BOUNDARY LAYER MACH NUMBER AND VELOCITY DISTRIBUTIONS FOR SPHERICAL ROUGHNESS

TUNNEL MACH NUMBER = 2.77 $\alpha = 1.25°$ $\xi = .00412$ in.

STATION 5			STATION 6			STATION 7		
x = 1.638 ft.			x = 1.971 ft.			x = 2.304 ft.		
P_o = 96.47 in. Hg.			P_o = 95.88 in. Hg.			P_o = 95.91 in. Hg.		
T_o = 117°F			T_o = 121°F			T_o = 121°F		
M_1 = 2.699			M_1 = 2.686			M_1 = 2.657		
y-in.	M	U/U_1	y-in.	M	U/U_1	y-in.	M	U/U_1
.0090	1.077	.5636	.0090	1.076	.5642	.0117	.947	.5097
.0114	1.087	.5679	.0109	1.104	.5759	.0147	.999	.5331
.0136	1.096	.5718	.0160	1.170	.6034	.0192	1.069	.5637
.0187	1.202	.6150	.0209	1.215	.6211	.0243	1.107	.5797
.0239	1.252	.6345	.0259	1.253	.6362	.0292	1.155	.5997
.0287	1.328	.6632	.0309	1.301	.6545	.0341	1.213	.6234
.0337	1.375	.6803	.0359	1.350	.6725	.0390	1.252	.6384
.0387	1.396	.6878	.0409	1.381	.6837	.0440	1.282	.6501
.0437	1.417	.6950	.0459	1.401	.6909	.0492	1.307	.6596
.0489	1.448	.7058	.0559	1.455	.7097	.0592	1.371	.6833
.0537	1.479	.7165	.0661	1.496	.7235	.0691	1.411	.6975
.0639	1.529	.7330	.0759	1.530	.7347	.0790	1.444	.7090
.0738	1.565	.7447	.0862	1.563	.7454	.0892	1.491	.7250
.0838	1.624	.7632	.0959	1.604	.7585	.0991	1.523	.7357
.0937	1.653	.7720	.1060	1.637	.7686	.1092	1.562	.7485
.1039	1.701	.7862	.1311	1.720	.7933	.1194	1.589	.7572
.1137	1.740	.7977	.1561	1.814	.8198	.1442	1.664	.7802
.1237	1.770	.8059	.1810	1.895	.8412	.1692	1.735	.8014
.1337	1.820	.8199	.2060	1.977	.8619	.1941	1.808	.8219
.1587	1.920	.8460	.2309	2.055	.8804	.2192	1.880	.8410

TABLE I (CONT'D)

BOUNDARY LAYER MACH NUMBER AND VELOCITY DISTRIBUTIONS FOR SPHERICAL ROUGHNESS

TUNNEL MACH NUMBER = 2.77 α = -1.25° ξ = .00412 in.

STATION 5 (Cont'd)	STATION 6 (Cont'd)	STATION 7 (Cont'd)
x = 1.638 ft.	x = 1.971 ft.	x = 2.304 ft.
P_o = 96.47 in. Hg.	P_o = 95.88 in. Hg.	P_o = 95.91 in. Hg.
T_o = 117°F	T_o = 121°F	T_o = 121°F
M_1 = 2.699	M_1 = 2.686	M_1 = 2.657

y-in.	M	U/U_1	y-in.	M	U/U_1	y-in.	M	U/U_1
.1837	2.009	.8680	.3309	2.370	.9456	.2443	1.950	.8591
.2087	2.104	.8900	.3809	2.509	.9714	.2945	2.092	.8929
.2337	2.194	.9096	.4309	2.614	.9888	.3444	2.232	.9233
.2587	2.286	.9284	.4809	2.658	.9957	.3941	2.367	.9503
.2837	2.379	.9463	.5309	2.675	.9983	.4441	2.488	.9722
.3337	2.542	.9751	.5809	2.680	.9990	.4942	2.574	.9867
.3837	2.645	.9918	.6309	2.680	.9990	.5441	2.623	.9946
.4337	2.679	.9971	.7309	2.686	1.0000	.5940	2.643	.9978
.4837	2.685	.9980				.6940	2.650	.9990
.5337	2.692	.9990				.7942	2.657	1.0000
.5837	2.697	.9997						
.6339	2.690	.9987						
.7337	2.699	1.0000						

TABLE I (CONT'D)

BOUNDARY LAYER MACH NUMBER AND VELOCITY DISTRIBUTIONS
FOR SPHERICAL ROUGHNESS

TUNNEL MACH NUMBER = 2.77 α = -1.25° ξ = .00412 in.

STATION 8

x = 2.638 ft.
P_o = 95.46 in. Hg.
T_o = 125°F
M_1 = 2.635

y-in.	M	U/U_1
.0135	.988	.5299
.0155	1.020	.5443
.0205	1.076	.5686
.0255	1.132	.5922
.0305	1.169	.6077
.0355	1.209	.6237
.0405	1.254	.6414
.0505	1.301	.6595
.0605	1.351	.6781
.0705	1.391	.6929
.0805	1.428	.7060
.0905	1.467	.7193
.1155	1.547	.7461
.1405	1.626	.7713
.1655	1.698	.7933
.1905	1.764	.8124
.2155	1.831	.8310
.2405	1.901	.8495
.2905	2.032	.8820
.3405	2.160	.9112
.3905	2.281	.9366
.4405	2.396	.9589
.4905	2.494	.9765
.5405	2.569	.9893
.5905	2.606	.9953
.6405	2.626	.9986
.6905	2.629	.9991
.7405	2.630	.9993
.8405	2.635	1.0000

TABLE II

TABULATION OF BOUNDARY LAYER CHARACTERISTICS FOR SPHERICAL ROUGHNESS ON THE FLAT PLATE AT MACH NO. 2.77

ξ = .00412 in. R_ξ = 2673.86 α = -1.25°

STATION	x (in.)	M_1	R_x	δ^*	θ	G	$H = \delta^*/\theta$	C_F
2	7.656	2.6985	4.97×10^6	.05888	.01203	.02124	4.8944	.003143
3	11.652	2.7019	7.57×10^6	.09230	.01896	.03364	4.8681	.003254
4	15.648	2.7022	10.165×10^6	.11455	.02410	.04332	4.7531	.003080
5	19.656	2.6985	12.77×10^6	.13656	.02917	.05275	4.6815	.002968
6	23.652	2.6861	15.36×10^6	.15747	.03393	.06122	4.6410	.002869
7	27.648	2.6566	17.96×10^6	.18561	.04005	.06855	4.6345	.002897
8	31.656	2.6347	20.65×10^6	.19532	.04290	.07708	4.5529	.002710
				SMOOTH PLATE				
				α = -1.25°				
3	11.652	2.7165	7.69×10^6	.06141	.01285	.02336	4.7790	.002206
4	15.648	2.7133	10.32×10^6	.07393	.01577	.02863	4.6880	.002016
5	19.656	2.7099	12.97×10^6	.09172	.01973	.03606	4.6488	.002008
6	23.652	2.6940	15.61×10^6	.10211	.02244	.04099	4.5504	.001898
7	27.648	2.6638	18.24×10^6	.11544	.02560	.04680	4.5094	.001852
8	31.656	2.6440	20.87×10^6	.12569	.02830	.05168	4.4413	.001788

TABLE III

DIMENSIONS OF SURFACE ROUGHNESS ON INSERTS TESTED*

Insert No.	Type	h	w	d	β
1	Smooth	—	—	—	—
2	Uniform Grain	No. 120 Aloxite; Mean Dia., ξ = 0.00728 in.			
3	"	No. 220 Aloxite; Mean Dia., ξ = 0.00612 in.			
4	"	No. 400 Aloxite; Mean Dia., ξ = 0.00094 in.			
5	"	No. 303 Optical Grit; Mean Dia., ξ = 0.00050 in.			
6	A	0.020	—	—	0
7	B	0.005	0.188	0.750	—
8	B	0.005	0.188	0.375	—
9	C	0.005	0.010	0.400	0
10	C	0.005	0.010	0.100	0
11	C	0.005	0.010	0.050	0
12	C	0.005	0.010	0.020	0
13	C	0.005	0.010	0.010	0
14	C	0.005	0.010	0.010	20
15	C	0.005	0.010	0.010	40
16	D	0.102	0.315	1.575	—

*See Fig. 4 for definition of symbols.

TABLE IV

BOUNDARY LAYER MACH NUMBER AND VELOCITY DISTRIBUTION FOR INSERTS TESTED

INSERT NO. 1 STA. NO. 8 x = 2.638 ft. M_1 = 2.241 p_o = 65.30 in. Hg. T_o = 150°F			INSERT NO. 1 STA. NO. 3 x = 0.971 ft. M_1 = 2.242 p_o = 65.36 in. Hg. T_o = 151°F			INSERT NO. 2 STA. NO. 8 x = 2.638 ft. M_1 = 2.231 p_o = 78.55 in. Hg. T_o = 152°F		
y-in.	M	U/U_1	y-in.	M	U/U_1	y-in.	M	U/U_1
.0090	1.084	.6163	.0090	1.106	.6262	.0090	0.746	.4481
.0111	1.101	.6241	.0103	1.146	.6441	.0114	0.771	.4615
.0131	1.106	.6264	.0124	1.228	.6798	.0134	0.803	.4786
.0180	1.154	.6479	.0147	1.273	.6987	.0182	0.861	.5088
.0232	1.231	.6814	.0193	1.295	.7078	.0232	0.902	.5297
.0280	1.309	.7137	.0243	1.342	.7267	.0337	0.997	.5766
.0382	1.345	.7282	.0343	1.439	.7643	.0434	1.070	.6112
.0480	1.389	.7455	.0446	1.521	.7943	.0534	1.115	.6319
.0580	1.448	.7679	.0544	1.580	.8150	.0732	1.204	.6713
.0779	1.509	.7903	.0648	1.670	.8451	.0932	1.268	.6984
.0980	1.557	.8073	.0743	1.707	.8569	.1134	1.327	.7226
.1184	1.611	.8259	.0944	1.836	.8962	.1335	1.377	.7425
.1382	1.675	.8470	.1147	1.971	.9339	.1535	1.430	.7628
.1580	1.721	.8617	.1345	2.064	.9579	.1732	1.478	.7808
.1779	1.768	.8765	.1544	2.145	.9777	.1932	1.526	.7982
.1980	1.810	.8889	.1743	2.202	.9909	.2332	1.619	.8304
.2230	1.871	.9067	.1945	2.226	.9964	.2737	1.707	.8592
.2480	1.924	.9215	.2244	2.233	.9979	.3132	1.796	.8867
.2731	1.976	.9356	.2546	2.234	.9983	.3532	1.880	.9112
.2979	2.025	.9484	.2844	2.235	.9984	.3934	1.963	.9341
.3230	2.075	.9610	.3845	2.237	.9988	.4532	2.077	.9636
.3481	2.121	.9723	.4845	2.238	.9991	.5132	2.160	.9837
.3980	2.187	.9879	.9740	2.242	1.0000	.5732	2.204	.9940
.4480	2.223	.9961				.6732	2.225	.9987
.4981	2.235	.9988				.7732	2.228	.9994
.5480	2.237	.9992				.8732	2.230	.9998
.6482	2.239	.9997				.9147	2.231	1.0000
.7480	2.240	.9999						
.8483	2.241	1.0000						

TABLE IV (CONT'D)

BOUNDARY LAYER MACH NUMBER AND VELOCITY
DISTRIBUTION FOR INSERTS TESTED

INSERT NO. 1 STA. NO. 8 x = 2.638 ft. M_1 = 2.242 P_o = 78.53 in. Hg. T_o = 151°F			INSERT NO. 1 STA. NO. 3 x = 0.971 ft. M_1 = 2.243 P_o = 78.23 in. Hg. T_o = 152°F			INSERT NO. 9 STA. NO. 8 x = 2.638 ft. M_1 = 2.244 P_o = 78.62 in. Hg. T_o = 152°F		
y-in.	M	U/U_1	y-in.	M	U/U_1	y-in.	M	U/U_1
.0090	1.074	.6115	.0090	1.126	.6351	.0090	1.088	.6176
.0107	1.141	.6419	.0113	1.192	.6642	.0110	1.105	.6254
.0127	1.170	.6548	.0135	1.242	.6856	.0160	1.182	.6597
.0178	1.218	.6756	.0185	1.290	.7056	.0211	1.262	.6938
.0225	1.263	.6946	.0235	1.350	.7298	.0262	1.287	.7042
.0328	1.338	.7252	.0285	1.400	.7493	.0361	1.352	.7304
.0428	1.396	.7480	.0385	1.481	.7797	.0461	1.417	.7556
.0529	1.441	.7651	.0485	1.549	.8041	.0560	1.444	.7658
.0727	1.511	.7908	.0587	1.623	.8295	.0760	1.517	.7925
.0927	1.570	.8116	.0685	1.688	.8508	.0962	1.586	.8167
.1127	1.624	.8299	.0885	1.811	.8887	.1160	1.633	.8325
.1329	1.675	.8468	.1085	1.928	.9221	.1360	1.681	.8482
.1527	1.723	.8620	.1285	2.040	.9517	.1560	1.731	.8641
.1927	1.815	.8901	.1485	2.108	.9686	.1963	1.823	.8920
.2329	1.908	.9167	.1886	2.222	.9933	.2360	1.910	.9165
.2727	1.990	.9389	.2285	2.234	.9980	.2760	1.993	.9393
.3127	2.068	.9590	.2685	2.235	.9982	.3160	2.072	.9595
.3527	2.137	.9758	.3685	2.231	.9973	.3560	2.141	.9763
.4127	2.207	.9921	.4686	2.239	.9991	.4160	2.212	.9928
.4727	2.235	.9984	.5686	2.241	.9996	.4760	2.235	.9979
.5327	2.240	.9996	.9277	2.243	1.0000	.5361	2.242	.9995
.6327	2.241	.9998				.6360	2.242	.9995
.9325	2.242	1.0000				.9302	2.244	1.0000

TABLE IV (CONT'D)

BOUNDARY LAYER MACH NUMBER AND VELOCITY DISTRIBUTION FOR INSERTS TESTED

INSERT NO. 3
STA. NO. 8
x = 2.638 ft.
M_1 = 2.235
P_o = 77.24 in. Hg.
T_o = 153°F

y-in.	M	U/U_1
.0090	0.648	.3937
.0104	0.672	.4071
.0123	0.708	.4269
.0173	0.811	.4823
.0229	0.895	.5256
.0274	0.943	.5496
.0373	1.024	.5889
.0474	1.095	.6220
.0575	1.145	.6447
.0775	1.228	.6808
.0972	1.284	.7043
.1175	1.341	.7275
.1374	1.396	.7491
.1574	1.449	.7692
.1874	1.524	.7966
.2173	1.595	.8214
.2473	1.666	.8451
.2776	1.735	.8671
.3074	1.805	.8884
.3374	1.867	.9066
.3673	1.929	.9239
.4173	2.029	.9505
.4674	2.115	.9720
.5175	2.175	.9862
.5675	2.208	.9938
.6175	2.224	.9975
.7175	2.232	.9992
.8175	2.233	.9995
.9560	2.235	1.0000

INSERT NO. 7
STA. NO. 8
x = 2.638 ft.
M_1 = 2.233
P_o = 77.53 in. Hg.
T_o = 153°F

y-in.	M	U/U_1
.0090	1.085	.6179
.0108	1.130	.6384
.0164	1.225	.6800
.0211	1.286	.7056
.0259	1.327	.7223
.0359	1.405	.7530
.0460	1.461	.7742
.0560	1.508	.7914
.0758	1.581	.8171
.0961	1.634	.8351
.1161	1.667	.8459
.1360	1.689	.8531
.1561	1.724	.8642
.1859	1.798	.8869
.2159	1.869	.9077
.2461	1.928	.9243
.2758	1.983	.9391
.3062	2.036	.9529
.3360	2.087	.9657
.3660	2.129	.9760
.4162	2.184	.9889
.4661	2.208	.9945
.5159	2.218	.9967
.6161	2.212	.9954
.7161	2.228	.9990
.8160	2.233	1.0000

INSERT NO. 8
STA. NO. 8
x = 2.638 ft.
M_1 = 2.244
P_o = 76.51 in. Hg.
T_o = 153°F

y-in.	M	U/U_1
.0090	1.114	.6295
.0107	1.152	.6466
.0128	1.198	.6667
.0178	1.285	.7034
.0227	1.341	.7261
.0279	1.373	.7387
.0376	1.451	.7685
.0481	1.491	.7832
.0581	1.532	.7979
.0779	1.579	.8144
.0978	1.626	.8303
.1176	1.654	.8396
.1377	1.684	.8493
.1578	1.728	.8633
.1878	1.804	.8865
.2177	1.872	.9063
.2480	1.890	.9113
.2778	1.969	.9330
.3080	2.020	.9464
.3377	2.068	.9586
.3677	2.120	.9713
.4177	2.201	.9904
.4677	2.225	.9958
.5677	2.242	.9996
.6178	2.218	.9942
.6679	2.228	.9965
.7678	2.243	.9998
.8697	2.244	1.0000

TABLE IV (CONT'D)

BOUNDARY LAYER MACH NUMBER AND VELOCITY
DISTRIBUTION FOR INSERTS TESTED

INSERT NO. 10			INSERT NO. 11			INSERT NO. 12		
STA. NO. 8			STA. NO. 8			STA. NO. 8		
x = 2.638 ft.			x = 2.638 ft.			x = 2.638 ft.		
M_1 = 2.256			M_1 = 2.241			M_1 = 2.239		
P_o = 76.97 in. Hg.			P_o = 76.35 in. Hg.			P_o = 76.23 in. Hg.		
T_o = 152°F			T_o = 152°F			T_o = 152°F		
y-in.	M	U/U_1	y-in.	M	U/U_1	y-in.	M	U/U_1
.0090	1.047	.5971	.0090	1.022	.5873	.0090	0.849	.5017
.0112	1.097	.6202	.0113	1.081	.6149	.0115	0.898	.5267
.0163	1.161	.6489	.0162	1.163	.6519	.0164	0.970	.5624
.0214	1.238	.6820	.0214	1.208	.6715	.0216	1.017	.5851
.0265	1.278	.6987	.0267	1.250	.6893	.0265	1.054	.6026
.0363	1.343	.7250	.0361	1.325	.7202	.0365	1.138	.6410
.0463	1.397	.7461	.0463	1.378	.7412	.0463	1.190	.6640
.0566	1.446	.7646	.0568	1.423	.7585	.0573	1.237	.6841
.0665	1.477	.7761	.0662	1.460	.7724	.0765	1.313	.7156
.0866	1.540	.7987	.0864	1.521	.7945	.0961	1.375	.7403
.1066	1.596	.8180	.1064	1.580	.8152	.1166	1.432	.7622
.1266	1.650	.8360	.1263	1.631	.8325	.1366	1.486	.7822
.1465	1.697	.8512	.1465	1.684	.8499	.1571	1.535	.7999
.1665	1.749	.8675	.1763	1.751	.8710	.1865	1.599	.8220
.1963	1.820	.8888	.2066	1.824	.8930	.2162	1.668	.8450
.2264	1.887	.9081	.2362	1.889	.9117	.2470	1.739	.8676
.2566	1.951	.9257	.2662	1.956	.9301	.2767	1.800	.8862
.2865	2.014	.9424	.2965	2.014	.9455	.3071	1.862	.9044
.3164	2.075	.9578	.3262	2.072	.9602	.3365	1.892	.9129
.3463	2.128	.9707	.2566	2.124	.9729	.3665	1.983	.9377
.3763	2.171	.9808	.4065	2.189	.9883	.4164	2.075	.9613
.4264	2.223	.9927	.4565	2.222	.9958	.4665	2.151	.9798
.4763	2.244	.9974	.5063	2.232	.9980	.5165	2.200	.9912
.5763	2.250	.9988	.6063	2.236	.9989	.5665	2.226	.9971
.6764	2.252	.9992	.7064	2.238	.9994	.6165	2.234	.9989
.9510	2.256	1.0000	.9525	2.241	1.0000	.7165	2.237	.9996
						.8165	2.238	.9999
						.9517	2.239	1.0000

TABLE IV (CONT'D)

BOUNDARY LAYER MACH NUMBER AND VELOCITY
DISTRIBUTION FOR INSERTS TESTED

INSERT NO. 13
STA. NO. 8
x = 2.638 ft.
M_1 = 2.239
P_o = 76.15 in. Hg.
T_o = 152°F

y-in.	M	U/U_1
.0090	0.862	.5083
.0112	0.891	.5231
.0130	0.926	.5436
.0150	0.957	.5560
.0199	1.021	.5870
.0250	1.072	.6109
.0359	1.143	.6432
.0448	1.205	.6704
.0555	1.247	.6883
.0652	1.291	.7066
.0850	1.357	.7332
.1051	1.418	.7569
.1252	1.477	.7789
.1450	1.528	.7975
.1652	1.575	.8138
.1949	1.648	.8385
.2250	1.718	.8610
.2551	1.790	.8832
.2853	1.856	.9026
.3153	1.925	.9220
.3450	1.989	.9393
.3746	2.047	.9543
.4250	2.135	.9759
.4748	2.198	.9895
.5257	2.221	.9959
.5749	2.231	.9982
.6749	2.239	1.0000
.7750	2.238	.9997
.9368	2.239	1.0000

INSERT NO. 4
STA. NO. 8
x = 2.638 ft.
M_1 = 2.235
P_o = 76.88 in. Hg.
T_o = 153°F

y-in.	M	U/U_1
.0090	0.825	.4897
.0111	0.852	.5037
.0130	0.880	.5180
.0180	0.964	.5600
.0231	1.024	.5890
.0281	1.070	.6106
.0379	1.143	.6438
.0480	1.205	.6711
.0584	1.255	.6983
.0680	1.296	.7093
.0880	1.366	.7574
.1085	1.428	.7614
.1281	1.478	.7800
.1480	1.536	.8009
.1680	1.588	.8191
.1981	1.663	.8442
.2282	1.737	.8678
.2582	1.805	.8885
.2882	1.875	.9089
.3180	1.940	.9270
.3480	2.004	.9441
.3981	2.101	.9686
.4481	2.184	.9884
.4980	2.211	.9946
.5480	2.225	.9978
.5980	2.229	.9986
.6980	2.232	.9993
.7980	2.235	1.0000

INSERT NO. 4
STA. NO. 3
x = 0.971 ft.
M_1 = 2.239
P_o = 77.95 in. Hg.
T_o = 153°F

y-in.	M	U/U_1
.0090	1.123	.6342
.0120	1.194	.6657
.0170	1.273	.6992
.0223	1.337	.7252
.0271	1.387	.7449
.0370	1.464	.7741
.0472	1.543	.8026
.0570	1.603	.8234
.0670	1.668	.8450
.0871	1.795	.8846
.1071	1.920	.9206
.1270	2.017	.9465
.1471	2.117	.9716
.1770	2.207	.9927
.2071	2.224	.9966
.2571	2.226	.9970
.2871	2.231	.9981
.3807	2.230	.9980
.9571	2.239	1.0000

TABLE IV (CONT'D)

BOUNDARY LAYER MACH NUMBER AND VELOCITY
DISTRIBUTION FOR INSERTS TESTED

INSERT NO. 5
STA. NO. 8
x = 2.638 ft.
M_1 = 2.241
P_o = 76.63 in. Hg.
T_o = 152°F

y-in.	M	U/U_1
.0090	0.979	.5667
.0116	1.016	.5844
.0164	1.099	.6252
.0214	1.163	.6519
.0269	1.204	.6698
.0365	1.267	.6965
.0465	1.313	.7154
.0564	1.360	.7342
.0765	1.479	.7794
.0965	1.498	.7863
.1164	1.559	.8080
.1366	1.614	.8269
.1666	1.706	.8570
.2006	1.745	.8692
.2314	1.848	.9000
.2615	1.919	.9201
.2914	1.985	.9379
.3215	2.046	.9537
.3715	2.136	.9759
.4216	2.172	.9844
.4718	2.229	.9974
.5215	2.237	.9992
.6215	2.239	.9997
.7215	2.239	.9997
.9568	2.241	1.0000

INSERT NO. 14
STA. NO. 8
x = 2.638 ft.
M_1 = 2.239
P_o = 76.74 in. Hg.
T_o = 150°F

y-in.	M	U/U_1
.0090	0.925	.5393
.0112	0.966	.5605
.0132	0.996	.5751
.0182	1.067	.6087
.0234	1.106	.6266
.0282	1.144	.6437
.0383	1.212	.6795
.0484	1.267	.6967
.0584	1.316	.7168
.0783	1.383	.7434
.0982	1.443	.7663
.1182	1.500	.7873
.1382	1.556	.8073
.1584	1.604	.8238
.1782	1.651	.8395
.2084	1.726	.863[illegible]
.2383	1.798	.8856
.2684	1.869	.9064
.2982	1.902	.9157
.3284	1.997	.9414
.3583	2.059	.9574
.4083	2.143	.9779
.4582	2.198	.9908
.5083	2.224	.9967
.5584	2.253	.9987
.6586	2.256	.9994
.7585	2.257	.9997
.8583	2.258	.9998
.9565	2.239	1.0000

INSERT NO. 15
STA. NO. 8
x = 2.638 ft.
M_1 = 2.238
P_o = 77.09 in. Hg.
T_o = 151°F

y-in.	M	U/U_1
.0090	0.951	.5433
.0110	0.961	.5581
.0129	1.000	.5771
.0191	1.083	.6162
.0242	1.121	.6335
.0291	1.156	.6492
.0391	1.226	.6796
.0491	1.282	.7031
.0591	1.328	.7218
.0789	1.394	.7478
.0992	1.456	.7713
.1192	1.511	.7914
.1389	1.564	.8102
.1694	1.638	.8353
.1991	1.710	.8587
.2289	1.779	.8801
.2589	1.848	.9005
.2891	1.914	.9192
.3192	1.978	.9366
.3493	2.040	.9527
.3791	2.096	.9667
.4291	2.170	.9844
.4791	2.212	.9941
.5292	2.228	.9977
.6292	2.235	.9995
.7289	2.237	.9997
.9560	2.238	1.0000

TABLE IV (CONT'D)

BOUNDARY LAYER MACH NUMBER AND VELOCITY DISTRIBUTION FOR INSERTS TESTED

INSERT NO. 16
STA. NO. 8
x = 2.638 ft.
M_1 = 2.226
p_o = 77.24 in. Hg.
T_o = 151°F

y-in.	M	U/U_1
.0090	0.878	.5181
.0111	0.906	.5323
.0161	0.962	.5602
.0210	1.018	.5873
.0261	1.051	.6030
.0361	1.081	.6169
.0460	1.117	.6334
.0661	1.167	.6558
.0860	1.210	.6746
.1060	1.246	.6899
.1360	1.286	.7066
.1660	1.322	.7214
.1962	1.392	.7334
.2261	1.373	.7417
.2562	1.399	.7518
.3061	1.447	.7700
.3560	1.507	.7922
.4059	1.580	.8179
.4560	1.670	.8481
.5059	1.769	.8794
.5562	1.870	.9093
.6060	1.959	.9340
.6560	2.032	.9533
.7063	2.093	.9686
.7564	2.144	.9810
.8064	2.183	.9902
.8561	2.213	.9970
.9060	2.226	1.0000

INSERT NO. 6
STA. NO. 8
x = 2.638 ft.
M_1 = 2.240
p_o = 77.86 in. Hg.
T_o = 150°F

y-in.	M	U/U_1
.0090	1.051	.6010
.0111	1.111	.6287
.0143	1.166	.6533
.0194	1.225	.6788
.0252	1.262	.6945
.0300	1.317	.7170
.0395	1.364	.7358
.0502	1.412	.7544
.0595	1.452	.7694
.0693	1.487	.7823
.0888	1.544	.8028
.1093	1.600	.8222
.1297	1.656	.8408
.1499	1.700	.8551
.1692	1.745	.8692
.1893	1.793	.8838
.2193	1.859	.9032
.2495	1.922	.9210
.2796	1.986	.9382
.3093	2.046	.9538
.3387	2.099	.9670
.3687	2.145	.9781
.3994	2.185	.9875
.4493	2.218	.9950
.4993	2.231	.9979
.5494	2.234	.9986
.5994	2.236	.9990
.6993	2.237	.9993
.7992	2.238	.9995
.9480	2.240	1.0000

TABLE IV (CONT'D)

BOUNDARY LAYER MACH NUMBER AND VELOCITY
DISTRIBUTION FOR INSERTS TESTED

INSERT NO. 1
STA. NO. 8
x = 2.638 ft.
M_1 = 2.243
p_o = 77.90 in. Hg.
T_o = 150°F

y-in.	M	U/U_1
.0090	1.044	.5974
.0110	1.047	.5989
.0135	1.114	.6297
.0182	1.196	.6660
.0232	1.250	.6891
.0282	1.282	.7024
.0386	1.361	.7342
.0482	1.408	.7525
.0582	1.449	.7680
.0782	1.513	.7914
.0982	1.573	.8125
.1182	1.628	.8312
.1382	1.676	.8470
.1682	1.750	.8704
.1982	1.818	.8909
.2282	1.888	.9111
.2582	1.951	.9284
.2882	2.014	.9451
.3182	2.071	.9596
.3485	2.125	.9728
.3782	2.169	.9833
.4282	2.217	.9943
.4782	2.238	.9990
.5282	2.240	.9995
.6282	2.241	.9997
.9562	2.243	1.0000

INSERT NO. 1
STA. NO. 3
x = 0.971 ft.
M_1 = 2.247
p_o = 77.05 in. Hg.
T_o = 151°F

y-in.	M	U/U_1
.0090	1.118	.6278
.0113	1.153	.6466
.0133	1.196	.6654
.0173	1.257	.6914
.0224	1.323	.7184
.0272	1.381	.7414
.0372	1.469	.7747
.0472	1.537	.7992
.0569	1.609	.8241
.0674	1.674	.8455
.0871	1.789	.8814
.1073	1.911	.9166
.1273	2.026	.9473
.1474	2.127	.9724
.1672	2.195	.9884
.1872	2.229	.9961
.2174	2.239	.9983
.2472	2.241	.9988
.2972	2.240	.9986
.3974	2.244	.9994
.9454	2.247	1.0000

TABLE V

SUMMARY OF DATA OBTAINED FROM INSERTS TESTED

Insert No.	θ_8 (in.)	R_8 x 10^{-6}	C_d	ξ (in.)	ξ/h	d/h	β (Degrees)
1	0.03180	16.299	0.00174	0	—	—	—
1	0.03098	19.635	0.00166	0	—	—	—
1	0.03142	19.517	0.00170	0	—	—	—
2	0.04858	19.745	0.00340	0.00728	1.0000	1.0000	—
3	0.04750	19.289	0.00330	0.00612	1.0000	1.0000	—
4	0.04062	19.199	0.00256	0.00094	1.0000	1.0000	—
5	0.03432	19.129	0.00198	0.00050	1.0000	1.0000	—
6	0.03218	19.528	0.00177	0	0	—	0
7	0.03129	19.387	0.00168	0	0	150.00	—
8	0.03212	19.027	0.00176	0	0	75.00	—
9	0.03120	19.592	0.00167	0	0	80.00	0
10	0.03212	19.071	0.00176	0	0	20.00	0
11	0.03271	19.058	0.00182	0.00063	0.1260	10.00	0
12	0.04367	19.045	0.00292	0.00437	0.8740	4.00	0
13	0.04103	19.024	0.00265	0.00310	0.6200	2.00	0
14	0.03817	19.259	0.00237	0.00193	0.3860	2.00	20
15	0.03789	19.311	0.00234	0.00188	0.3760	2.00	40
16	0.07703	19.466	0.00625	0.05512	0.5404	15.44	—

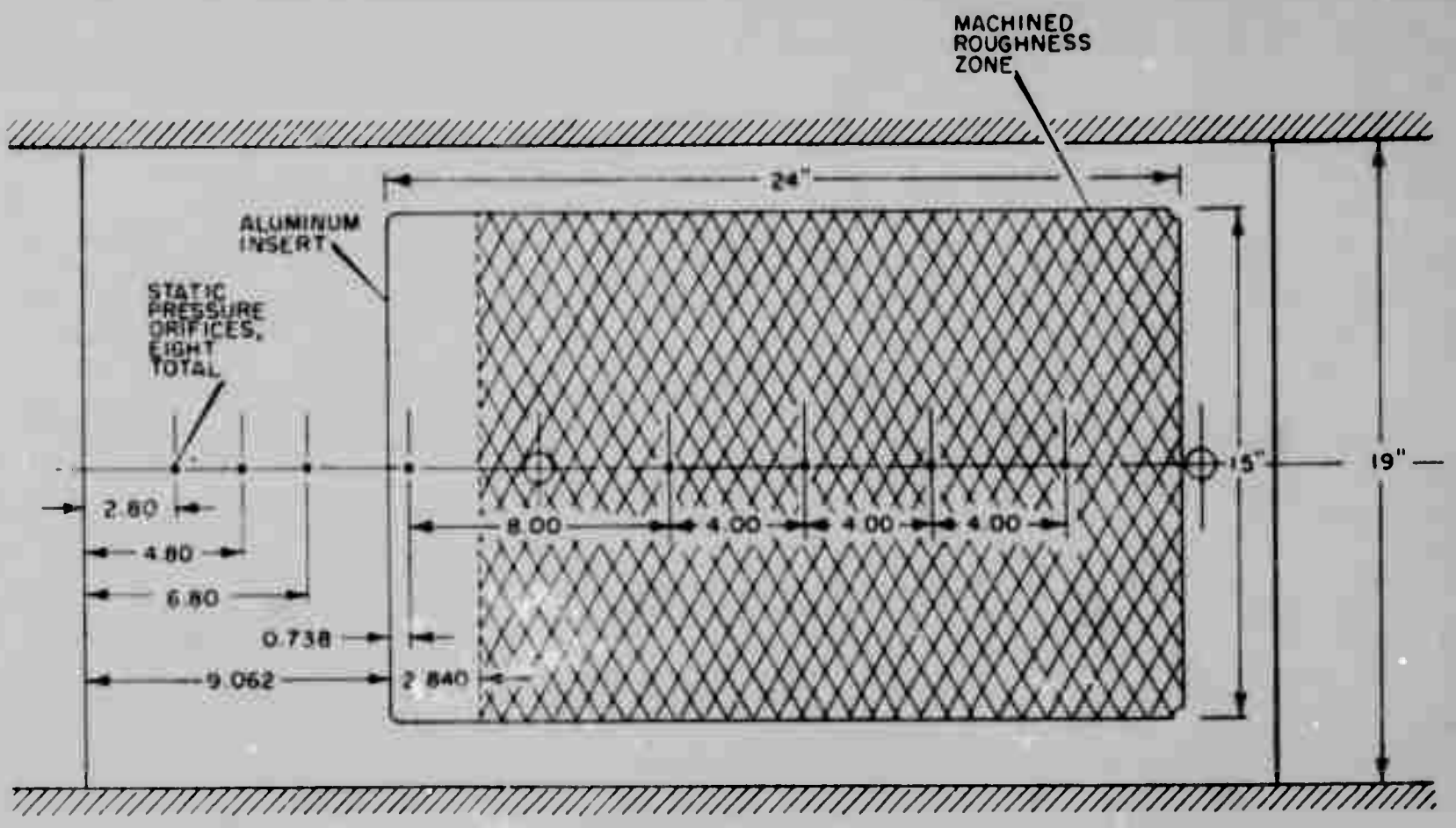

PLAN

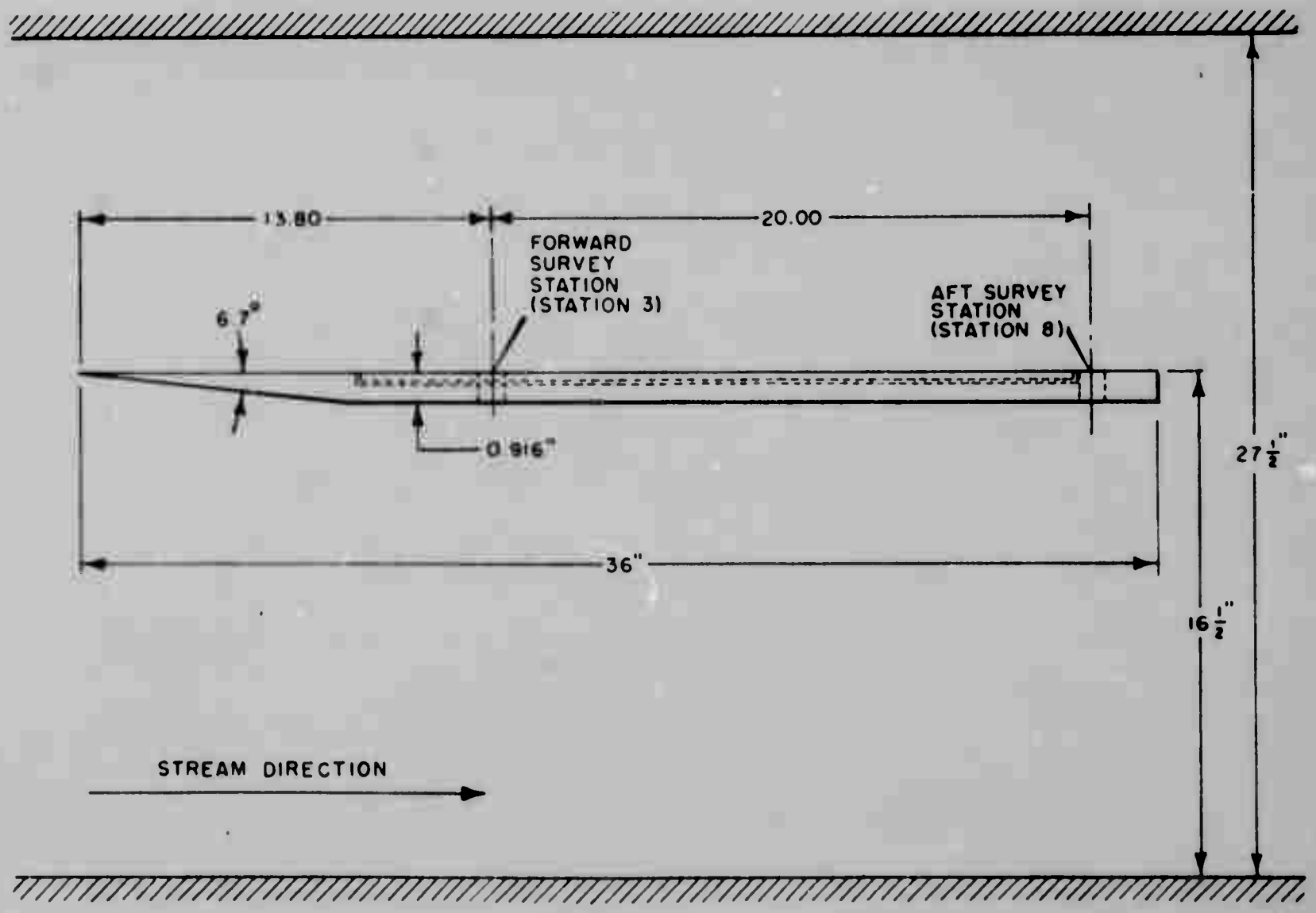

ELEVATION

FIG. 1 – SIGNIFICANT DIMENSIONS OF PLATE AND TUNNEL TEST SECTION

DRL – UT
DWG AA 2192
FWF – CLW
2 – 5 – 58

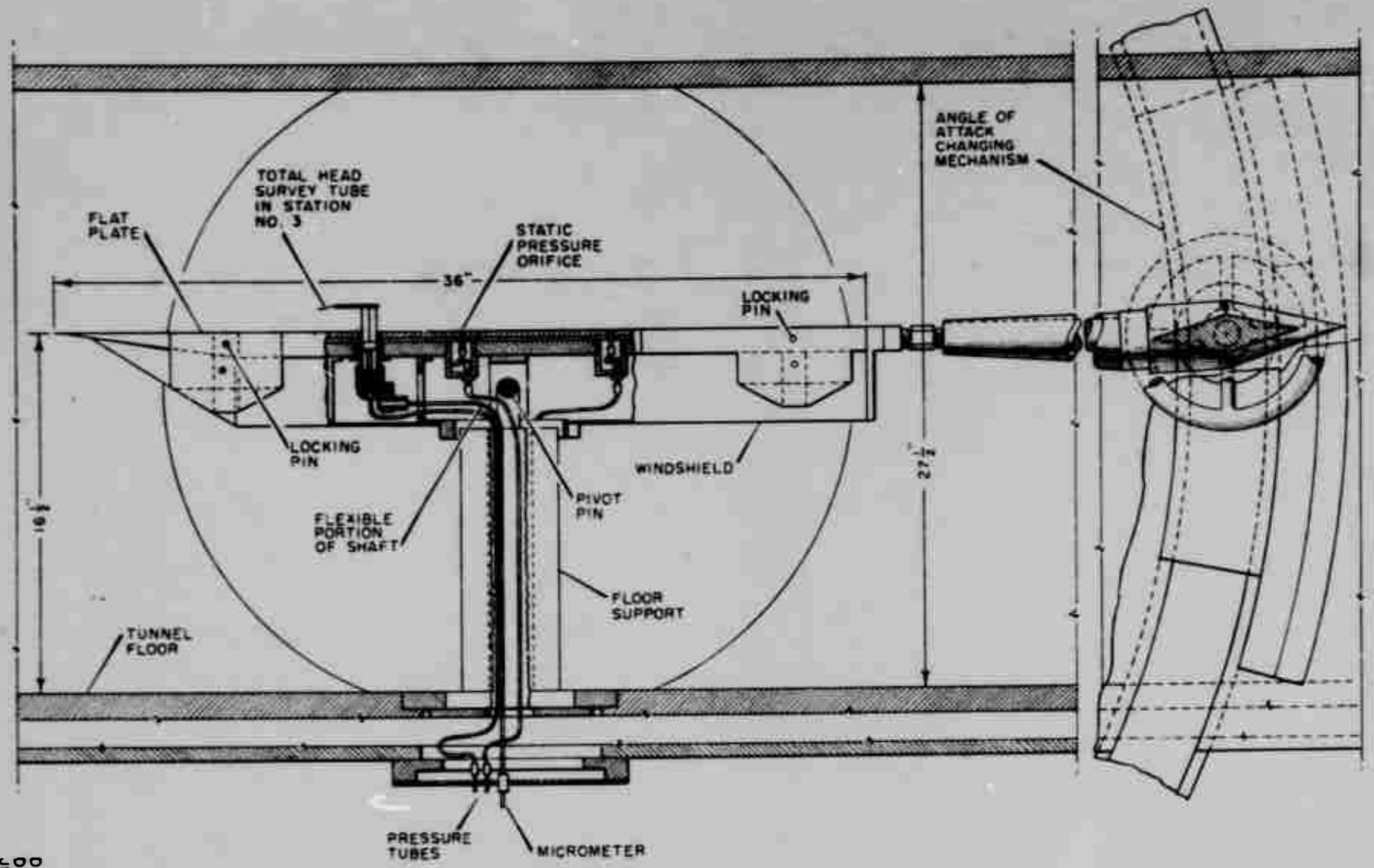

DRL-UT
DWG AA 2193
JLH 1CLW
2-4-58

FIG. 2 – BOUNDARY LAYER SURVEY PLATE – SIDE VIEW

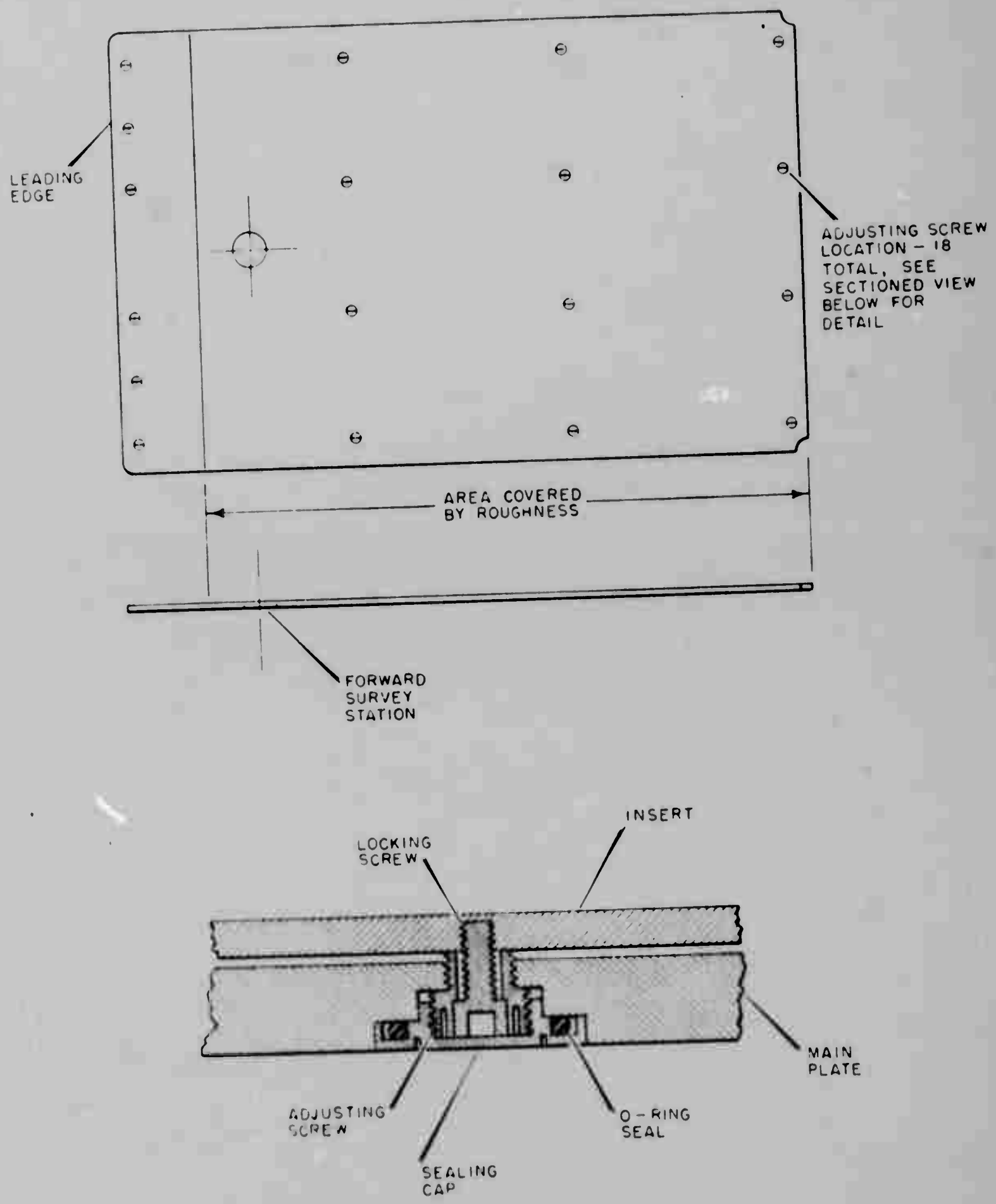

FIG. 3 – ROUGHNESS INSERT

DRL – UT
DWG AA 2194
FWF – CLW
2 – 6 – 58

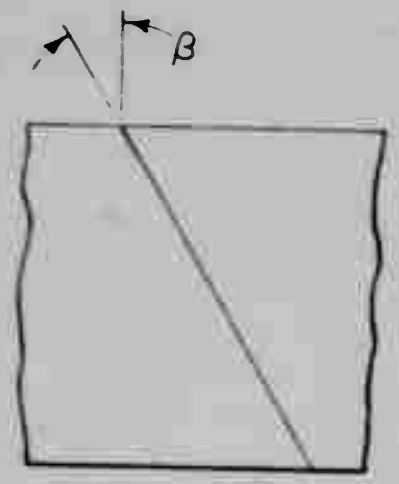

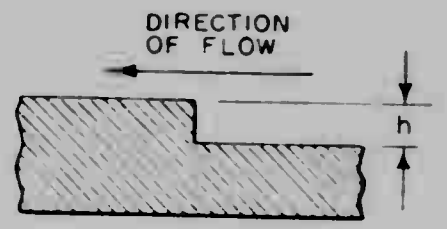

TYPE A

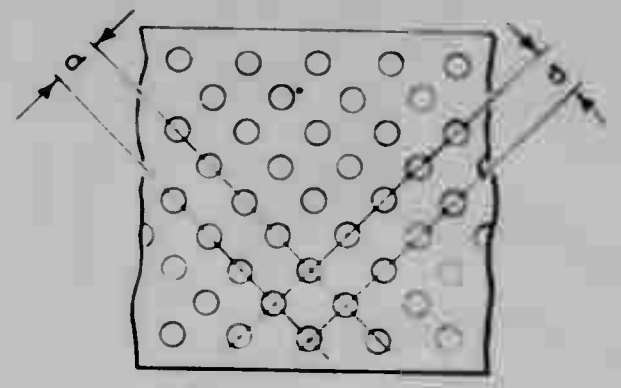

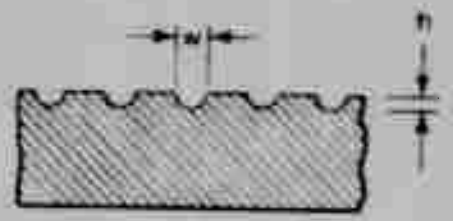

TYPE B

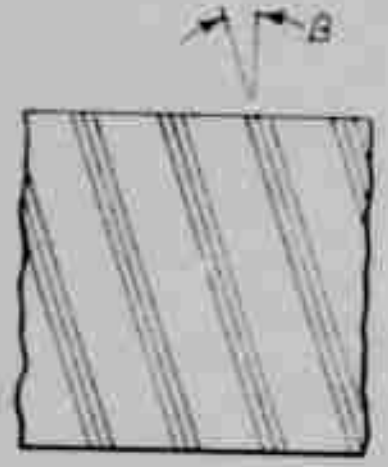

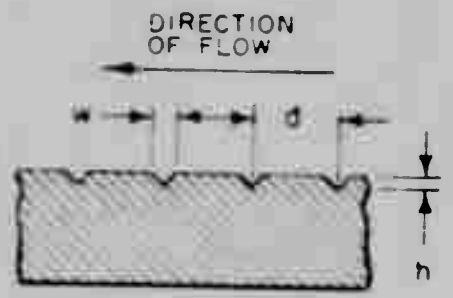

TYPE C

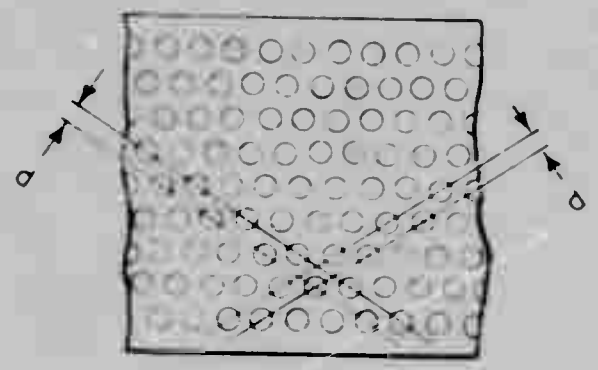

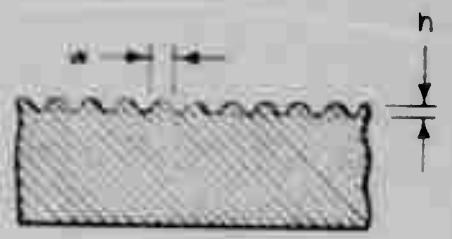

TYPE D

DRL - UT
DWG AA 2195
FWF - CLW
2 - 6 - 58

FIG. 4 – TYPES OF MACHINED ROUGHNESS TESTED

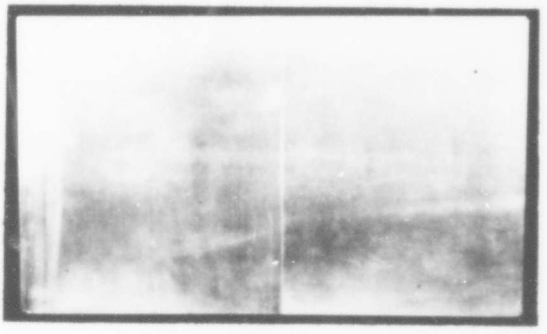

STEP-UP

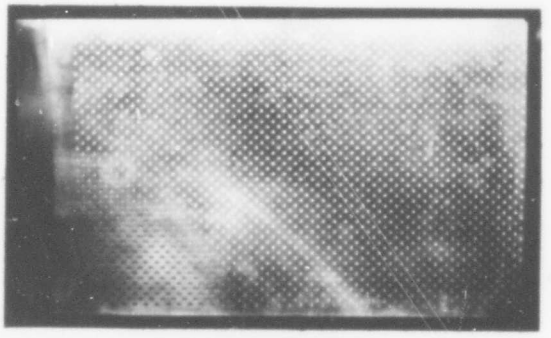

SPHERICAL INDENTURE

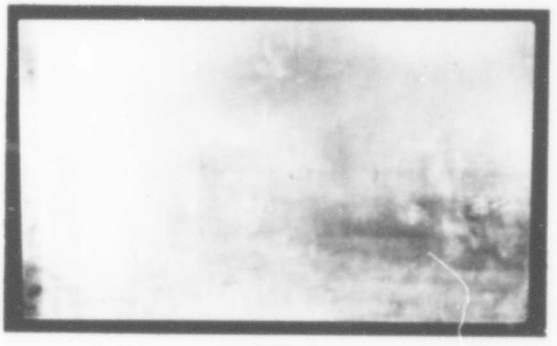

V-GROOVE
WITHOUT SWEEPBACK

V-GROOVE
WITH SWEEPBACK

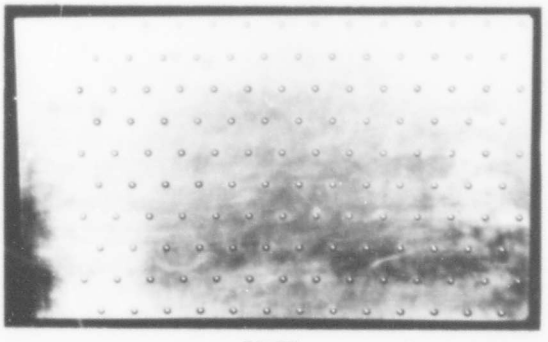

RIVET

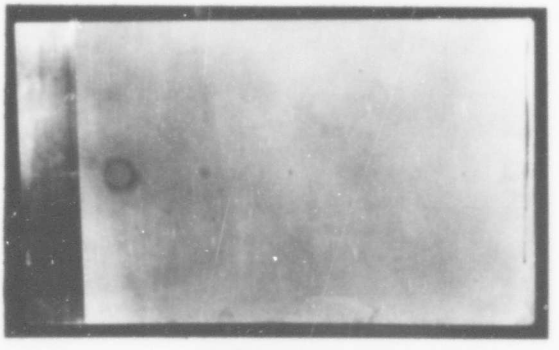

UNIFORM GRAIN

FIG. 5 - TYPICAL INSERT FOR EACH TYPE ROUGHNESS

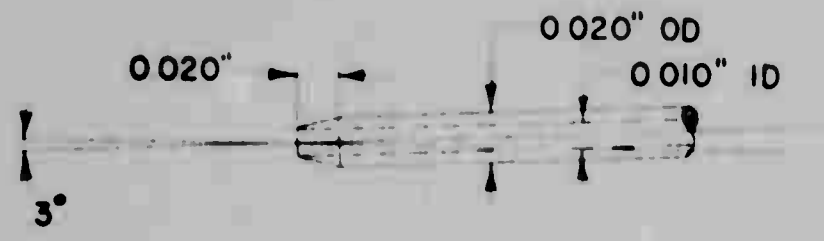

Approximate Dimensions Of Pitot Tube Tip

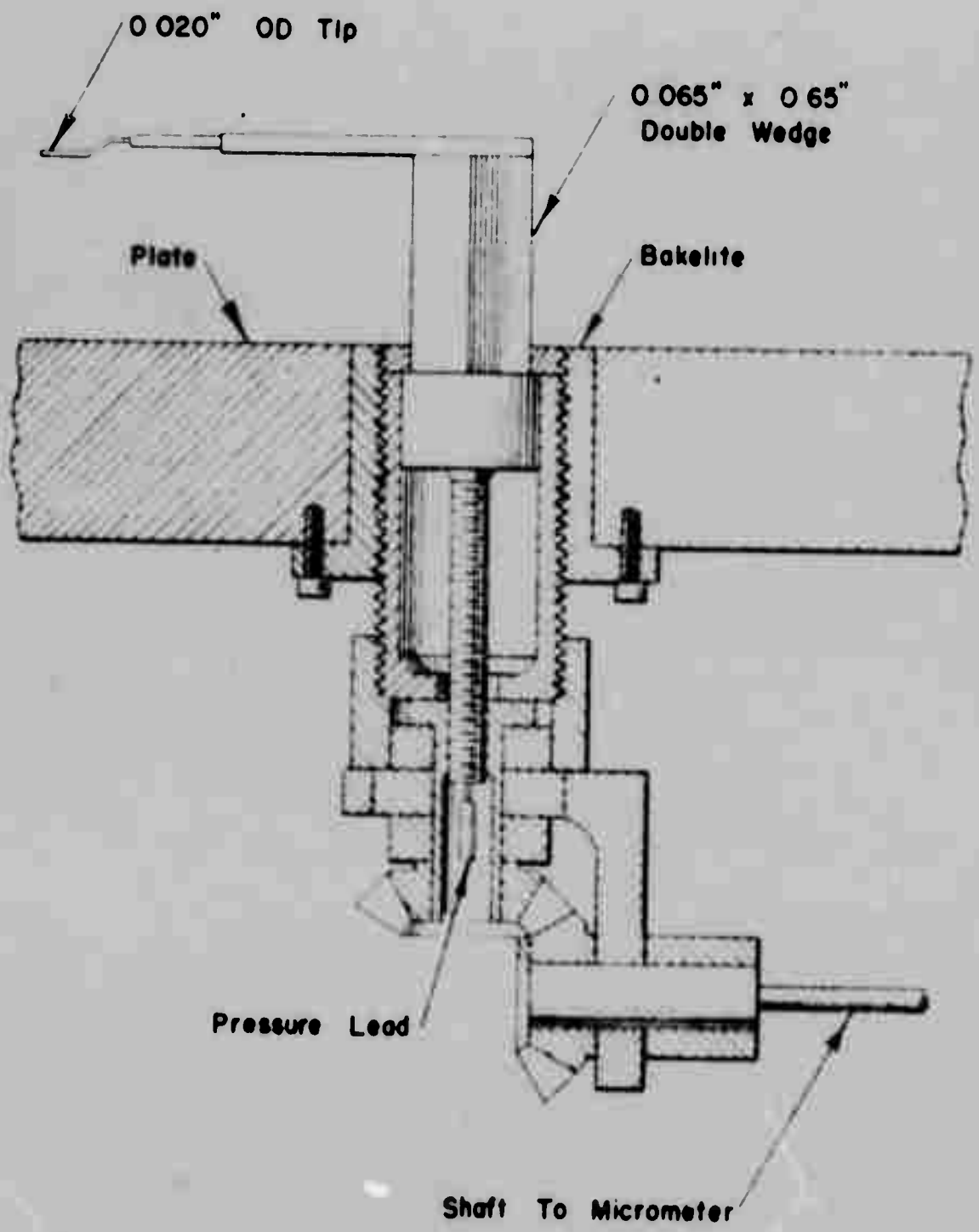

Fig. 6

PITOT TUBE

ORL—UT
DWG AA 779
REW—RWC
8—16—55

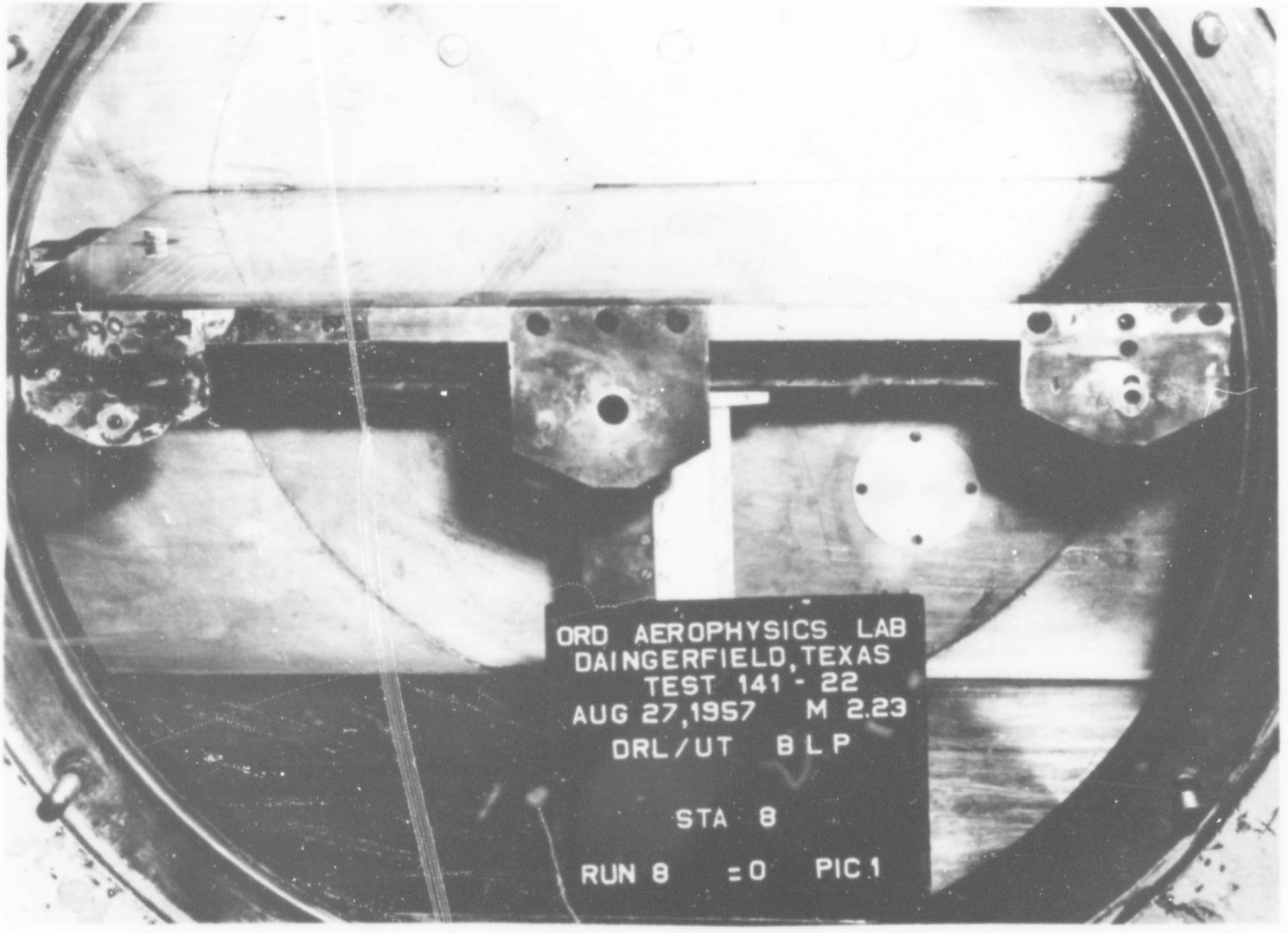

FIG. 7 – FLAT PLATE AND TYPICAL ROUGHNESS INSERT INSTALLED IN OAL WIND TUNNEL

PHOTOGRAPH COURTESY OF OAL/CVAC.

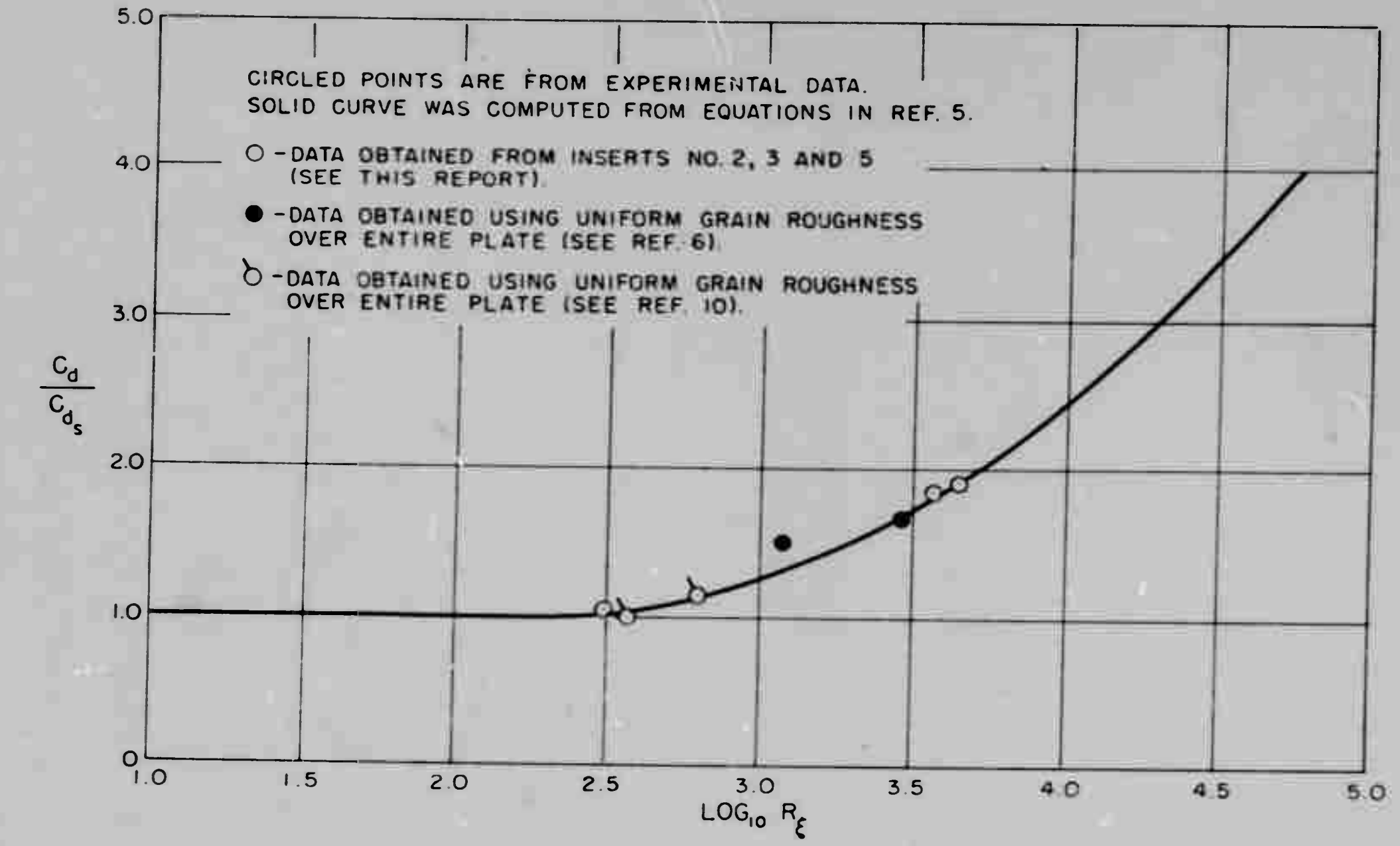

DRL - UT
DWG AA 2196
FWF - CLW
2 - 7 - 58

FIG. 8 - COMPARISON OF EXPERIMENTAL DRAG COEFFICIENTS WITH THEORY

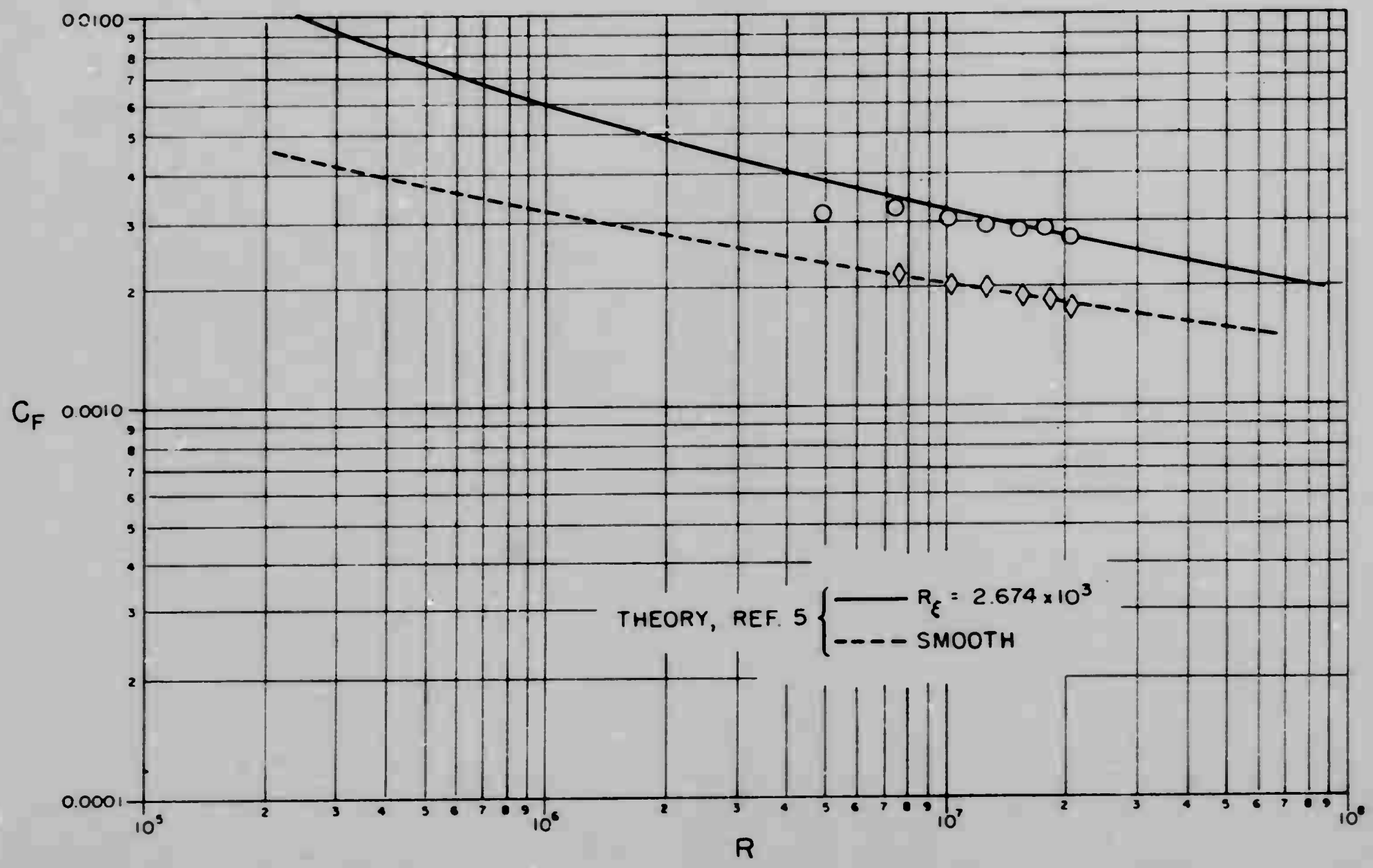

FIG. 9 — COMPARISON OF EXPERIMENTAL SKIN FRICTION COEFFICIENTS FOR SPHERICAL ROUGHNESS WITH THEORY

DRL - UT
DWG AA 2197
FWF - CLW
2 - 7 - 58

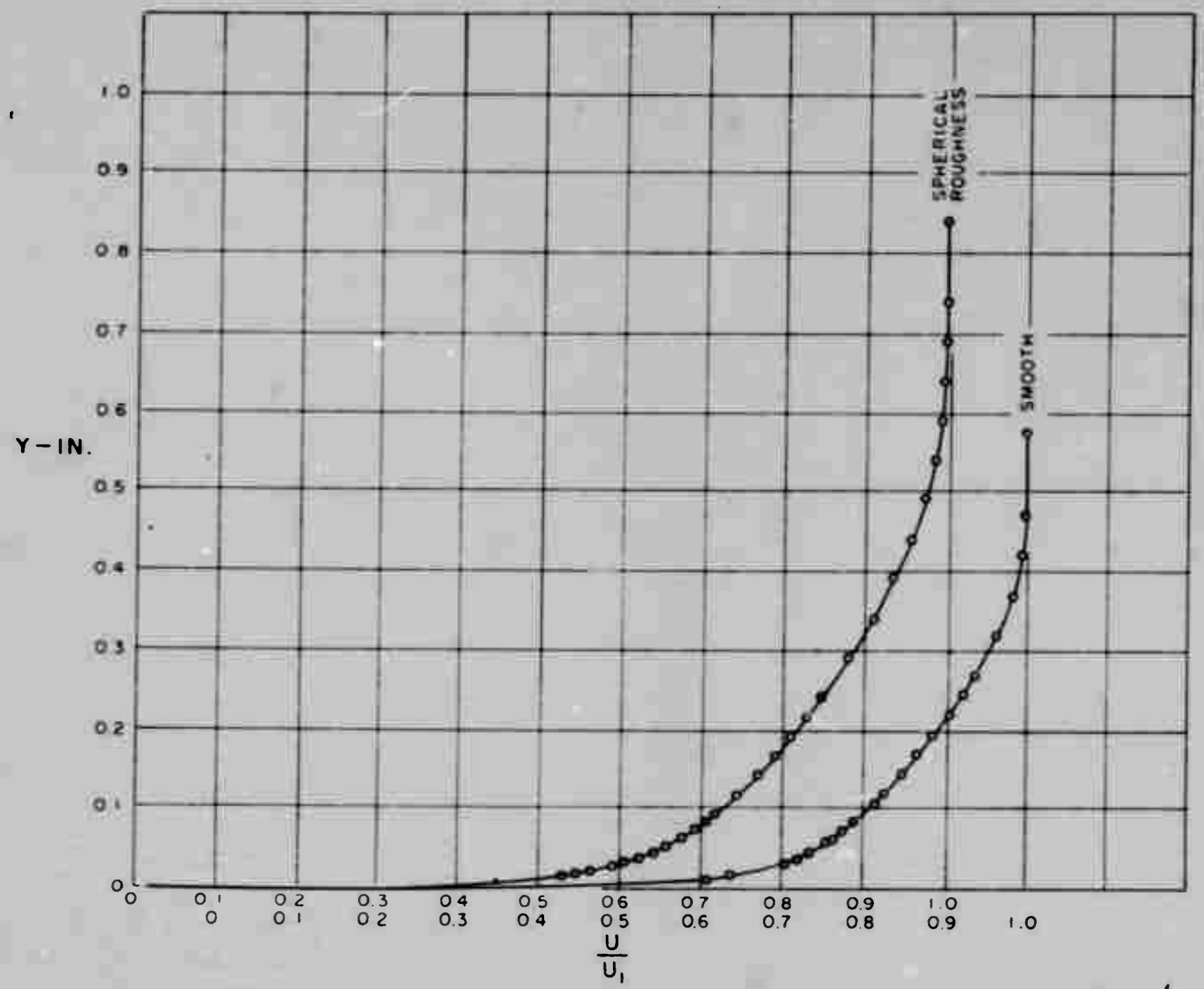

FIG. 10 — COMPARISON OF VELOCITY PROFILE FOR SPHERICAL ROUGHNESS

ORL — UT
DWG AA 2198
FWF — CLW
3-6-58

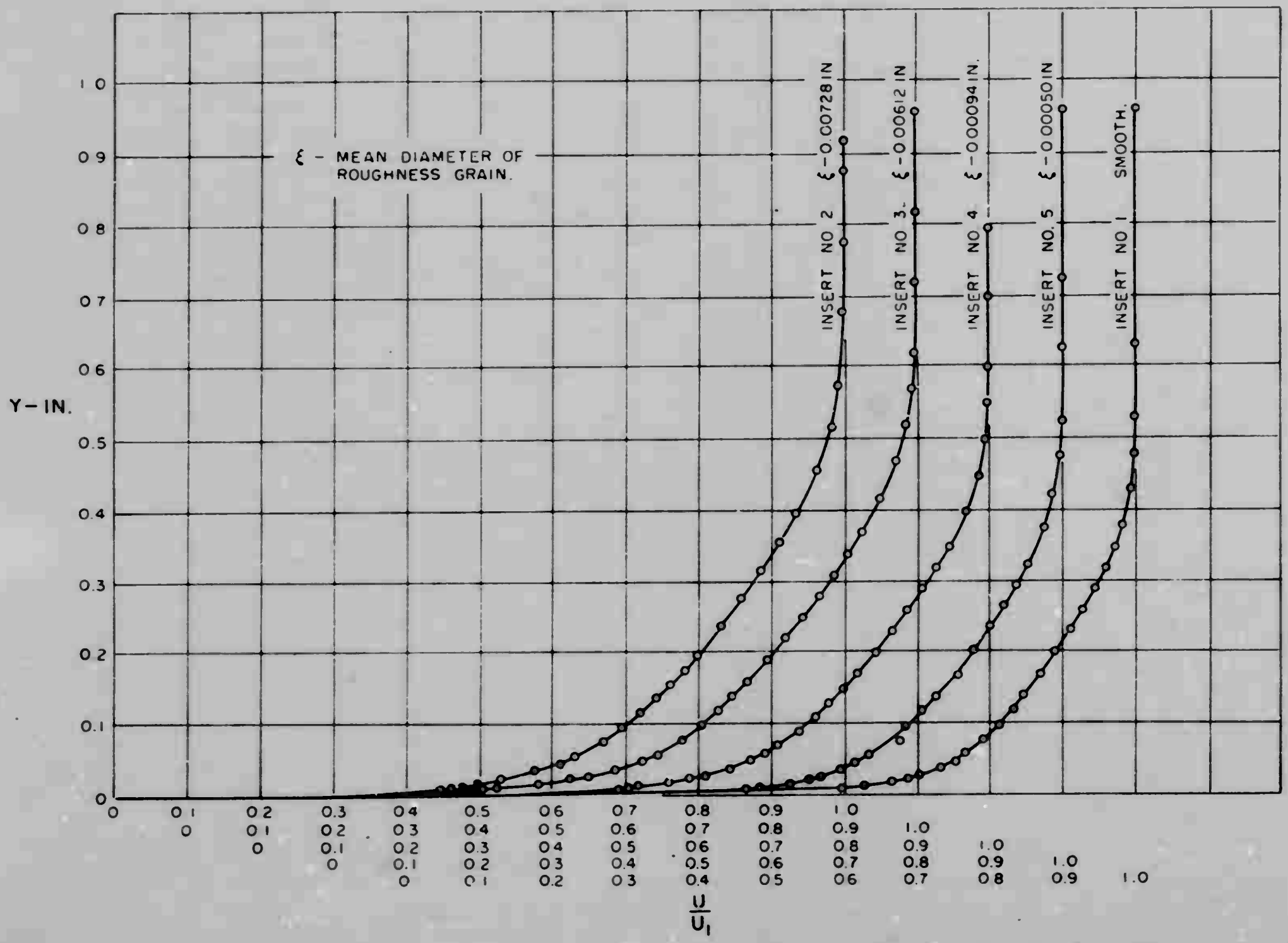

DRL - UT
DWG AA 2199
FWF - CLW
2 - 28 - 58

FIG. 11 - COMPARISON OF VELOCITY PROFILES FOR UNIFORM GRAIN ROUGHNESS

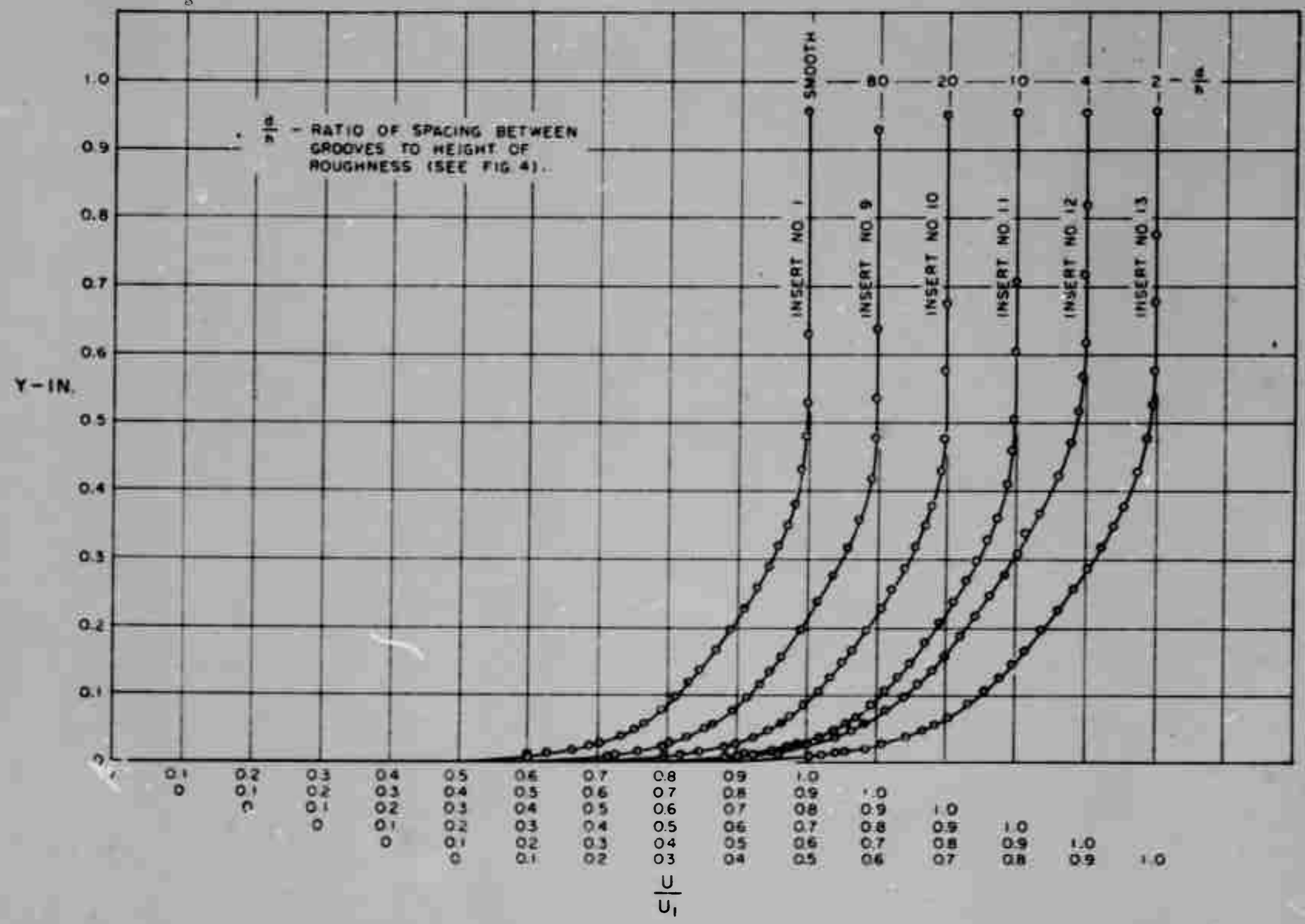

DRL - UT
DWG AA 2200
FWF - CLW
2 - 12 - 58

FIG. 12 - COMPARISON OF VELOCTY PROFILES FOR V-GROOVE ROUGHNESS AT VARIOUS DENSITIES

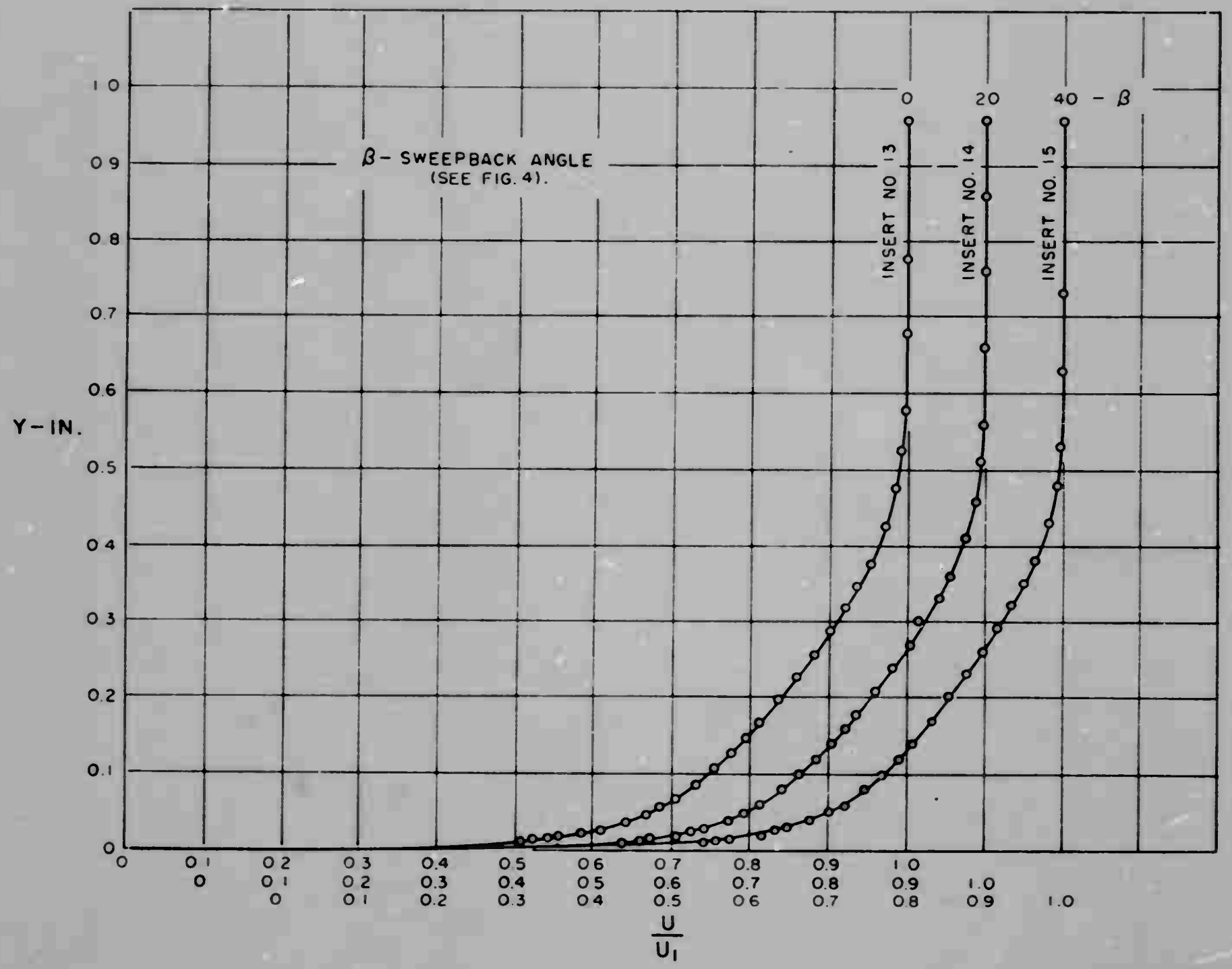

FIG. 13 - COMPARISON OF VELOCITY PROFILES FOR V-GROOVE ROUGHNESS AT VARIOUS SWEEPBACK ANGLES

DRL - UT
DWG AA2201
FWF - CLW
3 - 6 - 58

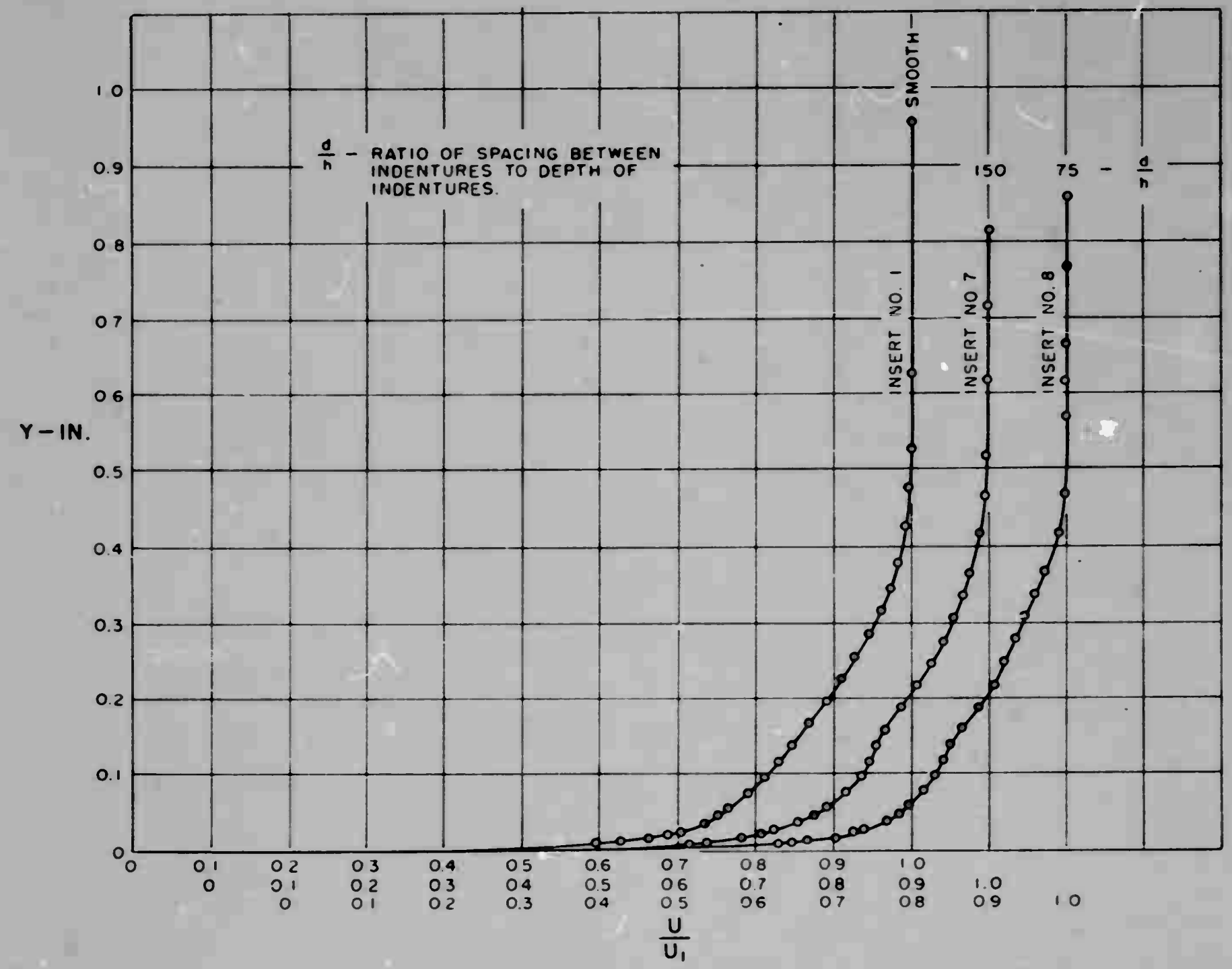

FIG. 14 – COMPARISON OF VELOCITY PROFILES FOR INDENTED SPHERICAL ROUGHNESS AT VARIOUS DENSITIES

DRL – UT
DWG AA2202
FWF – CLW
3 – 6 – 58

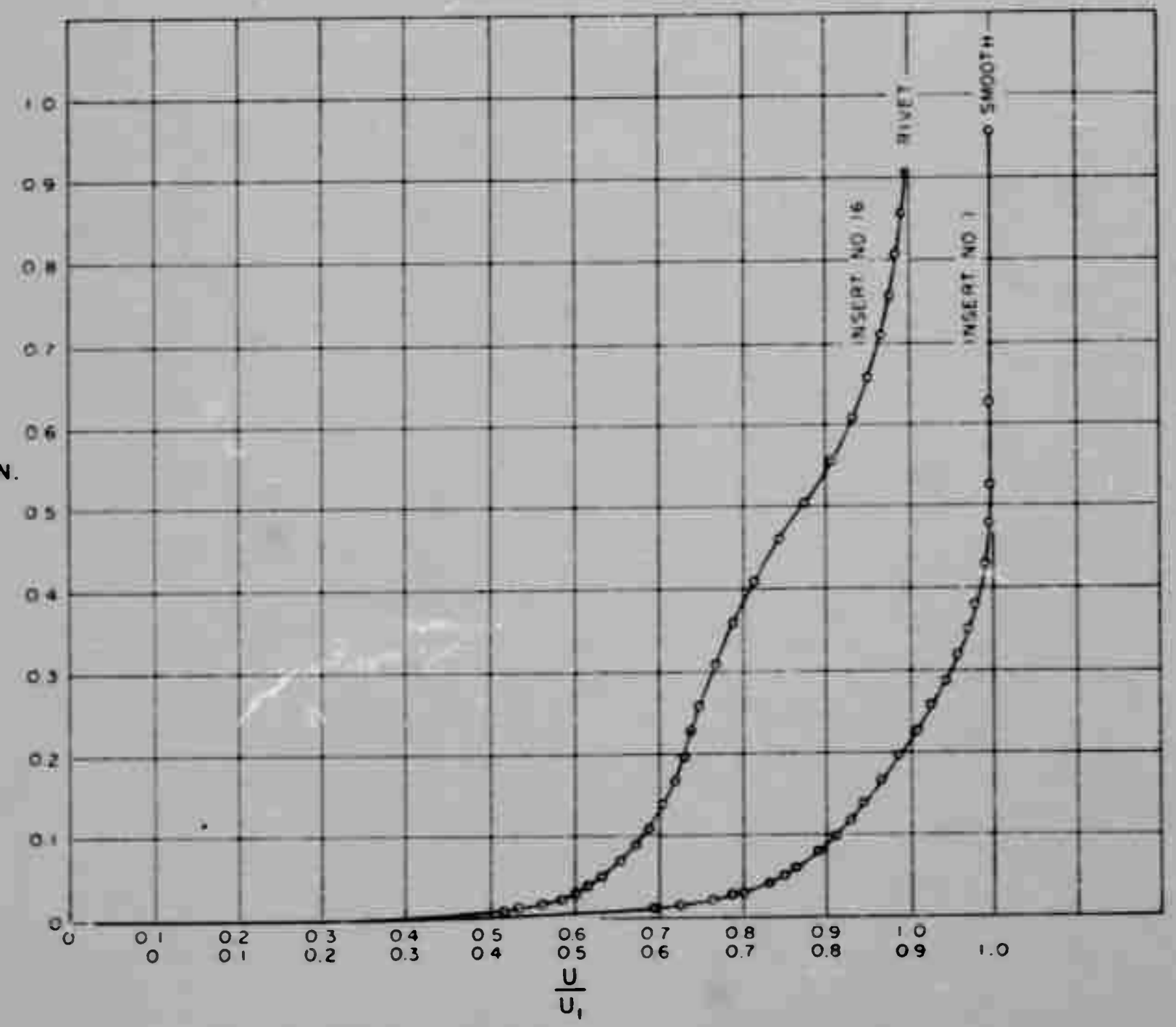

FIG. 15 — COMPARISON OF VELOCITY PROFILE FOR RIVET ROUGHNESS

DRL — UT
DWG AA 2203
FWF — CLW
3-6-58

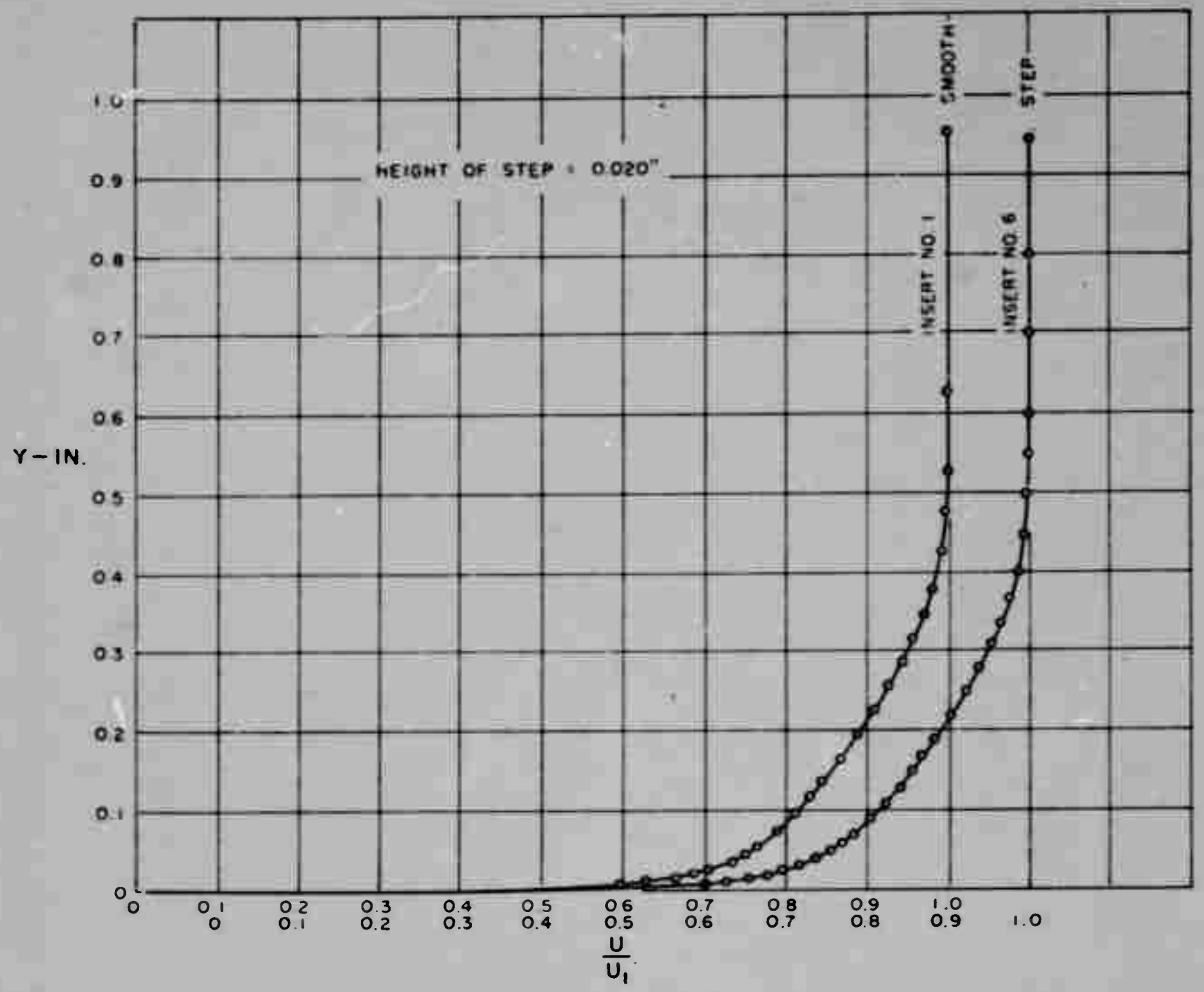

FIG. 16 – COMPARISON OF VELOCITY PROFILE BEHIND A STEP DISCONTINUITY

DRL – UT
DWG AA 2204
FWF – CLW
3 – 7 – 58

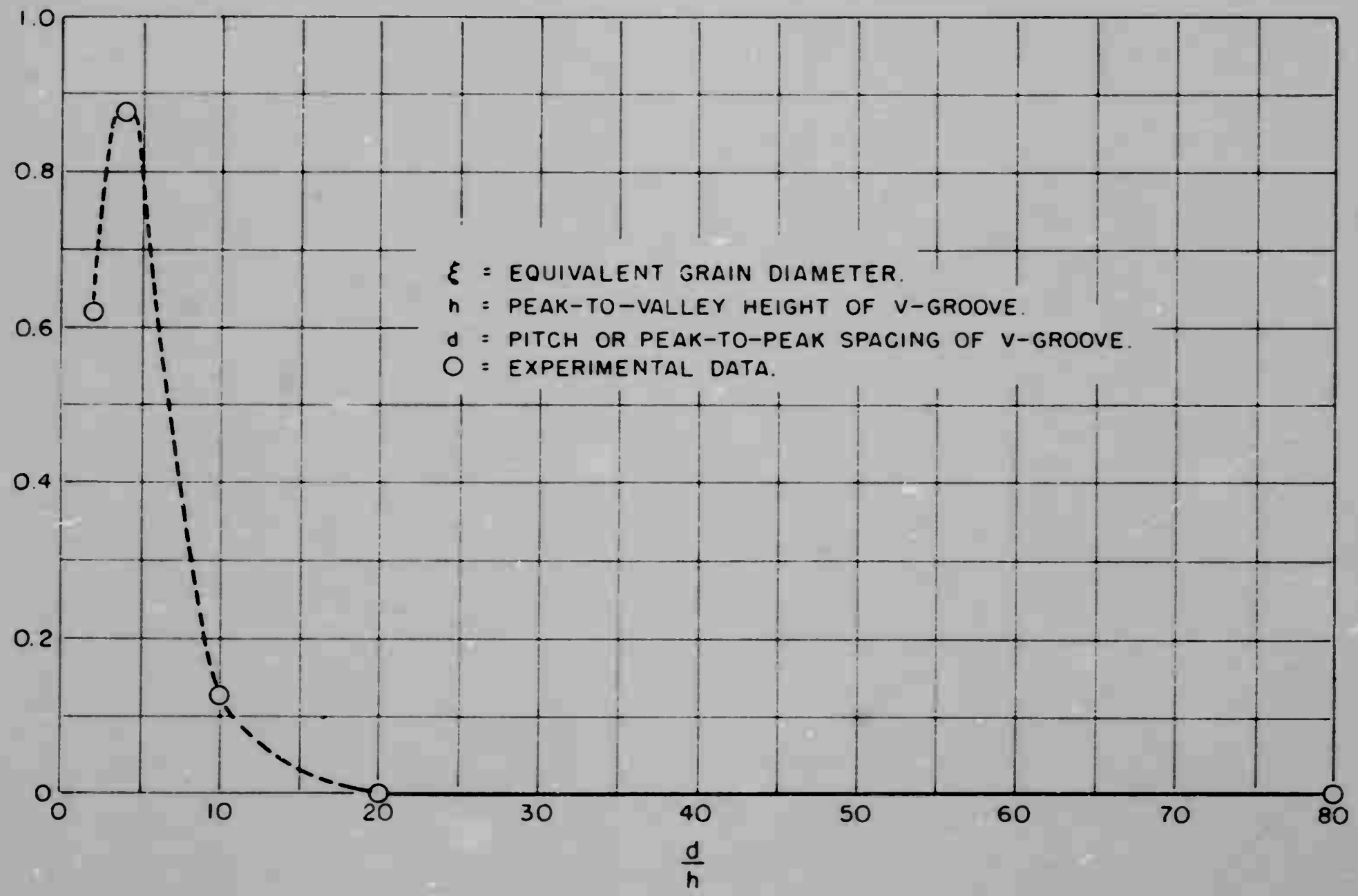

FIG. 17 – EQUIVALENT GRAIN DIAMETER FOR V-GROOVE ROUGHNESS AT VARIOUS DENSITIES OF DISTRIBUTION

ORL – UT
DWG AA 2205
FWF – CLW
2-7-58

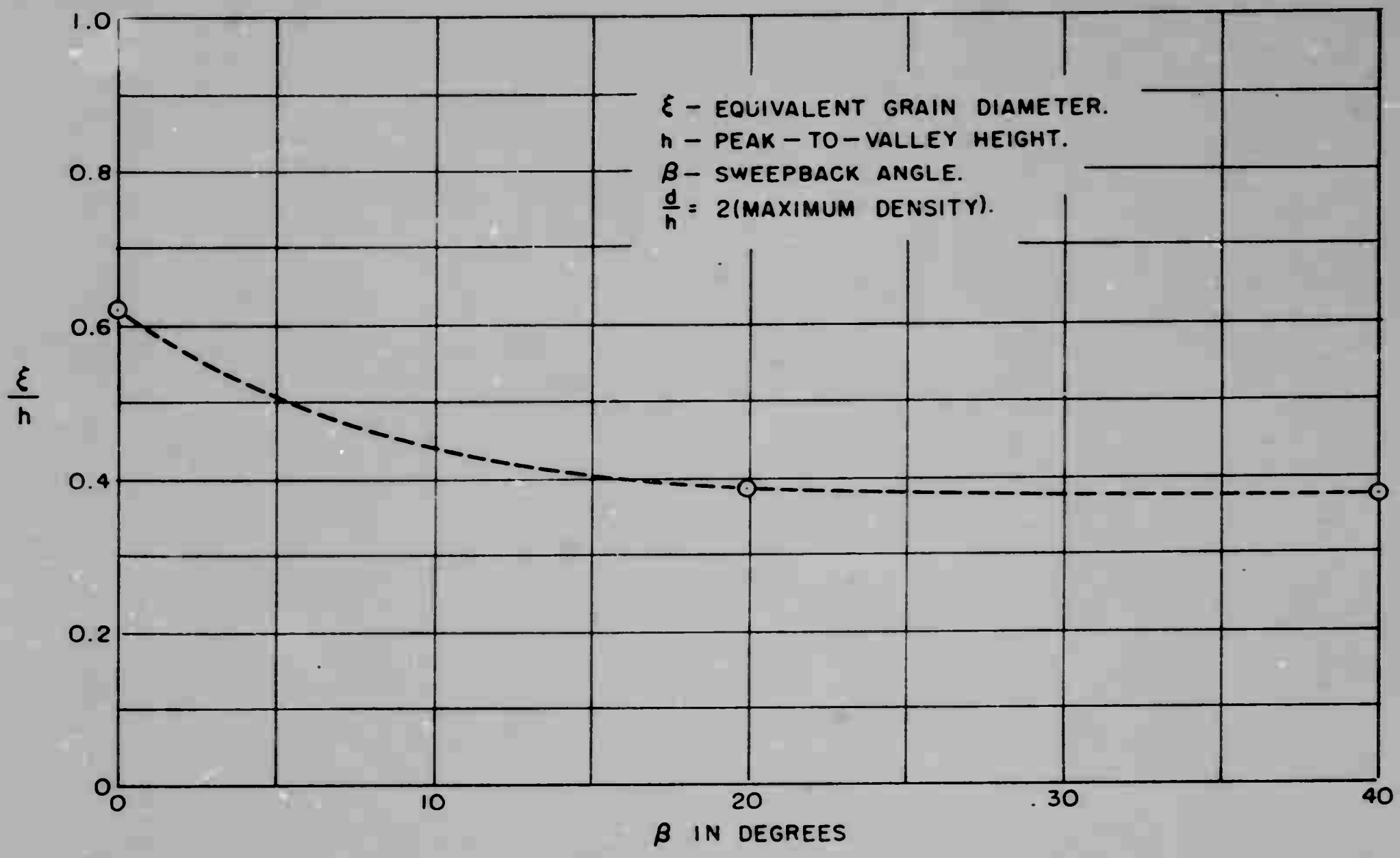

DRL – UT
DWG AA2206
FWF – CLW
2 – 14 – 58

FIG. 18 – EQUIVALENT GRAIN DIAMETER FOR V-GROOVE ROUGHNESS AT VARIOUS SWEEPBACK ANGLES